

# **Adaptive Brain-computer Interface using Motor-imagery EEG**

A thesis presented

by

Shih-Wei Lu

to

Institute of Computer Science and Engineering

College of Computer Science



in partial fulfillment of the requirements

for the degree of

Master

in the subject of

Computer Science

National Chiao Tung University

Hsinchu, Taiwan

2007

# **Adaptive Brain-computer Interface using Motor-imagery EEG**

Copyright © 2007

by

Shih-Wei Lu



## Abstract

Recently, the research of EEG-based Brain-computer Interface provides a new way of communication and control. In the existing BCI researches, we are interested in the motor-imagery based BCI systems. Nowadays this kind of BCI system is facing many challenges such as noises and inter-subject variability. There are many issues to study, the noise reduction, the adaptation between a BCI and a user, the feedback of the BCI, etc.

In this work, we studied the adaptation issue in the Brain-computer Interface based on the motor-imagery EEG. First, we want to construct a good spatial filter that suppresses the noises and enhances the power change in a motor-imagery task. We use Maximum Contrast Beamforming technique to construct the spatial filter. This technique has its ability to lower the nontarget noise and enhance the contrast between the active state and control state we define. We focus on the usability of this spatial filter and analyse its performance by applying a ROC curve analysis. In this work we show that this spatial filter has its effectiveness.

Furthermore, we applied the constructed spatial filter online. We designed a two-session online experiment with a visual feedback to study the adaptation and the biofeedback issues. We expect the user to adapt himself to the system by monitoring the visual feedback, and the system to adapt to the user by training a new spatial filter. The result tells us that the spatial filter is possible to work online, but the visual feedback somehow affects the ERS in the motor-imagery tasks.





## Acknowledgements





# Contents

<b>List of Figures</b>	<b>vii</b>
<b>List of Tables</b>	<b>ix</b>
<b>1 Introduction</b>	<b>1</b>
1.1 Motivation . . . . .	2
1.2 The Human Brain . . . . .	3
1.3 Electroencephalography . . . . .	4
1.3.1 What is Electroencephalography . . . . .	4
1.3.2 How to measure Electroencephalography . . . . .	4
1.3.3 Basic Analysis to Electroencephalography . . . . .	5
1.4 Brain-computer Interface . . . . .	8
1.5 Thesis Overview . . . . .	9
<b>2 Overview of Brain-computer Interface</b>	<b>11</b>
2.1 Categories of Brain-computer Interface systems . . . . .	12
2.2 Basic Components in BCIs . . . . .	12
2.3 Present-day BCI systems . . . . .	14
2.3.1 ERP-based BCI . . . . .	14
2.3.2 Motor-imagery based BCI . . . . .	15
2.4 Limitations . . . . .	16
2.5 Key-issues in BCI systems . . . . .	17
2.6 Thesis scope . . . . .	19
<b>3 Cortical activity analysis for BCI</b>	<b>21</b>
3.1 Main ideas . . . . .	22
3.2 Data acquisition and preprocessing . . . . .	22
3.3 Time-frequency analysis . . . . .	23
3.4 Spatial filtering . . . . .	24
3.4.1 Introduction . . . . .	25
3.4.2 Beamforming technique . . . . .	25

3.4.3	Maximum Contrast Beamformer . . . . .	29
3.5	Thresholding . . . . .	31
3.5.1	ROC curve analysis . . . . .	31
<b>4</b>	<b>Experiments</b>	<b>33</b>
4.1	Offline analysis . . . . .	34
4.1.1	Experiment setup . . . . .	34
4.1.2	Data analysis . . . . .	36
4.1.3	Experiment results . . . . .	37
4.2	Online feedback experiment . . . . .	54
4.2.1	Experiment setup . . . . .	54
4.2.2	Experiment results . . . . .	56
4.3	Observations . . . . .	57
<b>5</b>	<b>Discussion</b>	<b>59</b>
5.1	Spatial filter . . . . .	60
5.1.1	Stability of the spatial filter . . . . .	60
5.1.2	Different selection of control/active state . . . . .	64
5.1.3	Comparison between MCB and CSP . . . . .	66
5.1.4	Number of training trials . . . . .	68
5.2	Adaptation . . . . .	75
5.2.1	The system to user adaptation . . . . .	75
5.2.2	The user to system adaptation . . . . .	76
5.3	Limitations . . . . .	76
<b>6</b>	<b>Conclusions and Future Works</b>	<b>79</b>
6.1	Conclusions . . . . .	80
6.2	Future works . . . . .	81
	<b>Bibliography</b>	<b>85</b>

# List of Figures

1.1	The lobes of human brain . . . . .	3
1.2	The functions of different cortex areas . . . . .	4
1.3	EEG measuring devices . . . . .	5
1.4	The international 10-20 system . . . . .	6
1.5	The P300 ERP . . . . .	7
1.6	The procedure of observing ERD/ERS . . . . .	8
1.7	Movement related alpha ERD and ERS . . . . .	9
1.8	The general flowchart of a BCI . . . . .	10
2.1	Flowchart of proposed BCI . . . . .	20
3.1	Example of a time-frequency map . . . . .	24
3.2	The concept of spatial filtering . . . . .	25
3.3	ROC curve analysis . . . . .	31
4.1	Experiment paradigm . . . . .	35
4.2	Time-Frequency map of Subject A, Experiment 1. . . . .	38
4.3	ERD/ERS curve of Subject A, Experiment 1. . . . .	38
4.4	Time-Frequency map of Subject A, Experiment 2. . . . .	39
4.5	ERD/ERS curve of Subject A, Experiment 2. . . . .	39
4.6	Time-Frequency map of Subject A, Experiment 3. . . . .	40
4.7	ERD/ERS curve of Subject A, Experiment 3. . . . .	40
4.8	Time-Frequency map of Subject A, Experiment 4. . . . .	41
4.9	ERD/ERS curve of Subject A, Experiment 4. . . . .	41
4.10	ROC curve analysis of Subject A, imagery session 1 and 2 . . . . .	42
4.11	ROC curve analysis of Subject A, imagery session 3 and 4 . . . . .	42
4.12	Time-Frequency map of Subject B, Experiment 1. . . . .	44
4.13	ERD/ERS curve of Subject B, Experiment 1. . . . .	44
4.14	Time-Frequency map of Subject B, Experiment 2. . . . .	45
4.15	ERD/ERS curve of Subject B, Experiment 2. . . . .	45
4.16	Time-Frequency map of Subject B, Experiment 3. . . . .	46
4.17	ERD/ERS curve of Subject B, Experiment 3. . . . .	46

4.18	Time-Frequency map of Subject C, Experiment 1. . . . .	48
4.19	ERD/ERS curve of Subject C, Experiment 1. . . . .	48
4.20	Time-Frequency map of Subject C, Experiment 2. . . . .	49
4.21	ERD/ERS curve of Subject C, Experiment 2. . . . .	49
4.22	Time-Frequency map of Subject C, Experiment 5. . . . .	50
4.23	ERD/ERS curve of Subject C, Experiment 5. . . . .	50
4.24	Time-Frequency map of Subject D, Experiment 1. . . . .	52
4.25	ERD/ERS curve of Subject D, Experiment 1. . . . .	52
4.26	Time-Frequency map of Subject D, Experiment 2. . . . .	53
4.27	ERD/ERS curve of Subject D, Experiment 2. . . . .	53
4.28	Online experiment paradigm design . . . . .	54
4.29	Online experiment visual feedback . . . . .	54
4.30	ERD/ERS curve of Subject A, Experiment 1. . . . .	56
5.1	Different result when choosing different active/control state . . . . .	65
5.2	C4 channel data compared to CSP and MCB filtered data, subject A im- agery session 1 and 2 . . . . .	69
5.3	C4 channel data compared to CSP and MCB filtered data, subject A im- agery session 3 and 4 . . . . .	70
5.4	Trial number vs. filter performance analysis . . . . .	71
5.5	Result of different onset time of the visual feedback . . . . .	75



# List of Tables

4.1	Results of subject A imagery movement . . . . .	43
5.1	Correlation coefficients between different sessions, wrist real movement, subject A . . . . .	61
5.2	Correlation coefficients between different sessions, wrist imagery movement, subject A . . . . .	62
5.3	Correlation coefficients between different tasks, subject A . . . . .	63
5.4	Correlation coefficients between different subjects . . . . .	64
5.5	Results of different selection of control/active states, subject A real movement	72
5.6	Results of different selection of control/active states, subject A imagery movement . . . . .	73
5.7	Trial number analysis using dataset 4 of subject A . . . . .	74
5.8	Trial number analysis using dataset 3 of subject A . . . . .	74





# Chapter 1

## Introduction



In this first chapter we give some background knowledge to this thesis. We briefly introduce from the human brain to Electroencephalography to Brain-computer Interfaces. In section 1.2 we introduce the structure of a human brain and the different functions of cortex areas. In section 1.3 we give some introduction to Electroencephalography (EEG), so called brain wave. The measurement way, some basic analyses and researches are presented. In section 1.4 we give a brief introduction to Brain-computer Interfaces (BCI). The detail of BCI systems will be provided in the next chapter.

## 1.1 Motivation

There are a lot of patients suffering from the paralyzed body. Disorders such as Spinocerebellar Ataxia (SCA) and Amyotrophic Lateral Sclerosis (ALS) are motor-disabled. These diseases make the patients unable to communicate with the external world through the normal pathway. They can't talk or move their fingers to click a button.

As the time is different now, we start to think about the other pathways between human and a computer. That is, a Brain-computer Interface. A Brain-computer interface is defined as a communication system that does not depend on the brains normal output pathways of peripheral nerves and muscles. Nowadays researchers use Electroencephalogram, so called brain wave, as a source to communicate and control. The users can use a Brain-computer interface to communicate with the outside world without using any real movement. So if this technique successes, it indeed helps lots of motor-disabled people. Even if those are not paralyzed, the BCI system may provide some assistance to some works, like monitoring a pilot's fatigue to avoid accident, or monitoring a child's brain waves to train his concentration.

So researchers keep doing researches on EEG and BCI. The more we discover about the human brain, the more people we may help in the future.

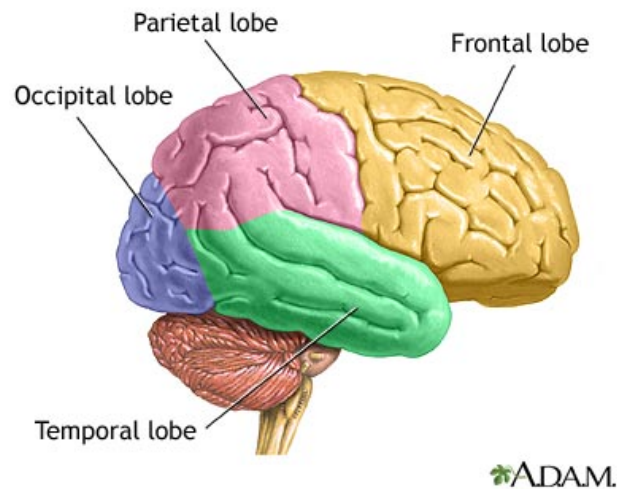


Figure 1.1: The lobes of human brain. [6]

## 1.2 The Human Brain

The human brain can be divided into four structures: cerebral cortex, cerebellum, brain stem, hypothalamus and thalamus. The one that related to BCIs is the cerebral cortex. The cerebral cortex can be divided in two hemispheres, left and right. And each hemisphere can be further divided into four lobes. The four lobes are frontal lobe, parietal lobe, temporal lobe, and occipital lobe, as figure 1.1 shows. The cerebral cortex is responsible for many complicated functions like mental calculating, language learning, visual stimulus processing, or motor movement. The different areas in the cerebral cortex are responsible for different functions. As figure 1.2 shows, these different areas of cerebral cortex are marked with different colors, indicating its responsible functions. For instance, the motor area is located at about parietal lobe. It's responsible for all the movement of the body. These informations are very important when doing researches on a EEG based BCI system. We observe the EEG from different locations on the head according to that area's representative function. For instance, we observe mainly the EEG from the channels located on the top (parietal) of the head when we are doing motor-related experiments, and we observe mainly the channels on the back (occipital) of the head when we are researching about visual stimulus.

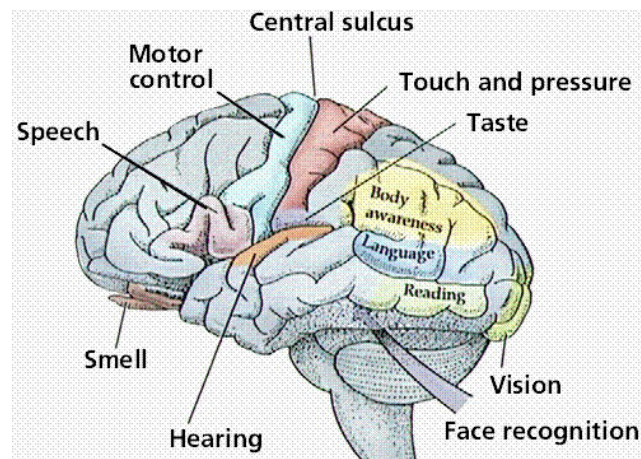


Figure 1.2: The functions of different cortex areas. [4]

## 1.3 Electroencephalography

### 1.3.1 What is Electroencephalography

Electroencephalography. There exists various non-invasive techniques to monitor the brain activity such as functional Magnetic Resonance Imaging (fMRI), magnetoencephalography (MEG), and Electroencephalography (EEG). EEG is used to measure the electrical activity of the brain. This activity is generated by billions of nerve cells, called neurons. Each neuron is connected to thousands of other neurons, and the neurons send action potentials to other neurons when they are communicating. When we measure the EEG, we actually are measuring the combined electrical activity of millions of neurons on the cerebral cortex because the potential of a single neuron is too small to be measured.

### 1.3.2 How to measure Electroencephalography

How to measure human EEG and record it for analysis? A typical EEG measuring device consists of several components, including EEG electrode cap that receives the electrical activity from the scalp, EEG amplifier that amplifies the signal, computers that record the data, and monitors that give the subjects visual cues. The devices are shown in figure 1.3.

The EEG signal has a good temporal resolution, but it has a poor spatial resolution,



Figure 1.3: EEG measuring devices. From right to left is the EEG amplifier and the electrode cap.

which depends on the electrode number of an EEG electrode cap. The electrode layout on an EEG electrode cap has an international standard called the international 10-20 system, as figure 1.4 shows. When we are measuring EEG, we often put some single electrodes surrounding the eye. This is used to measure the electrical activity of eye movement and eye blinking, which is called EOG. This EOG contaminates the EEG signal badly, so by measuring it we can remove the trials that were affected. This processing is called EOG rejection.

When we use an EEG electrode cap to measure EEG, we have to fill each electrode with the electrolyte gel using a blunt needle. This makes the electrodes contact the scalp and lower the impedance. In an EEG experiment we often wait until all the electrodes have an impedance lower than 5k ohm before we start the signal acquisition.

### 1.3.3 Basic Analysis to Electroencephalography

There are some basic EEG analyses, mainly described here as time domain and frequency domain analysis.

#### Time domain analysis

Usually we use time domain analysis to observe an Event-related Potential (ERP). An ERP is a potential change in the EEG when a particular event or stimulus occurs. The

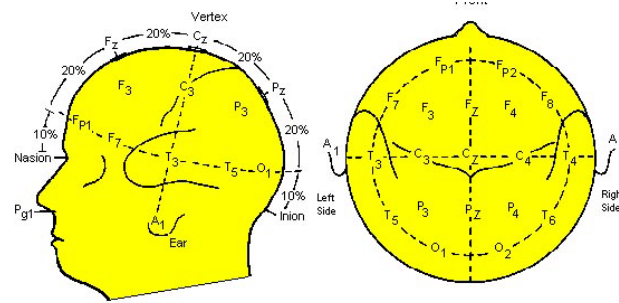


Figure 1.4: The international 10-20 system. The 10 and 20 means 10% and 20% distance in the left figure. The channels are named as a capital letter followed by a number. The capital letter 'F' is for 'Frontal', 'C' is for 'Central', 'P' is for 'Parietal', 'O' is for 'Occipital', and 'T' is for 'Temporal'. The numbers are odd on the left sphere and even on the right sphere. [5]

potential change is time-locked and phase-locked, it is a very small potential change and can not be easily observed in a single trial. So we have to average a few trials to observe it. Because of the time-locked and phase-locked characteristic, by the averaging technique we can eliminate the random noise and enhance the signal-to-noise ratio (SNR). That is the common technique to observe an ERP.

There are some well-known ERPs, including P100 in the Visual-evoked Potential (VEP), P300, N400, and Audio-evoked Potential (AEP). The P300 means a positive potential change occurs 300ms after the particular stimulus, as figure 1.5. In section 2.3.1 we will introduce more about the application on BCIs using ERPs.

### Frequency domain analysis

In addition to the ERPs in time domain analysis, we can observe Event-related Synchronization (ERS) and Event-related Desynchronization (ERD) in the frequency domain. When we are observing ERD and ERS, we have to observe a specific frequency band, like alpha band (8-12Hz) or beta band (around 20Hz). The ERD and ERS indicate the power changes of the frequency band. While ERD means the power decreasing and ERS means the power increasing.

The ERD/ERS analysis has a general procedure as figure 1.6 shows.

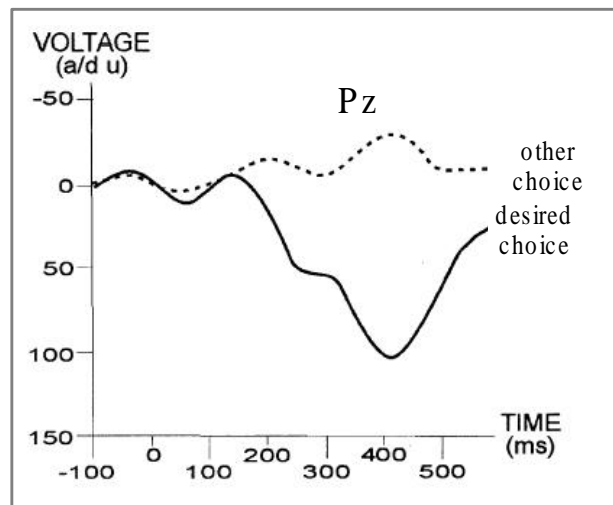


Figure 1.5: The P300 ERP. 300ms after the particular stimulus, there is a positive potential change in the time domain. This figure is a result of averaging. [3]

1. First we apply a bandpass filter with a specific frequency band to the data.
2. Calculate the mean of the filtered data over all trials.
3. Subtract the mean from the filtered data in step1.
4. We do the squaring on the time domain amplitude samples from the previous step over all trials.
5. Average over time samples from the step4.
6. Obtain ERD/ERS by calculating the percentage relative to the power of the baseline interval.

Then we can see the power change and the change rate clearly after these procedures.

There are some well-known ERD/ERS. For example, the movement related ERD and ERS. It is known by now that during the movement there is an alpha ERD, and after the movement terminates there is a beta ERS. In this thesis we are mainly observing this phenomenon. Figure 1.7 shows the movement related alpha ERD and ERS. In addition to observing the ERD/ERS curve, we can analyse the data using wavelet transform to obtain a



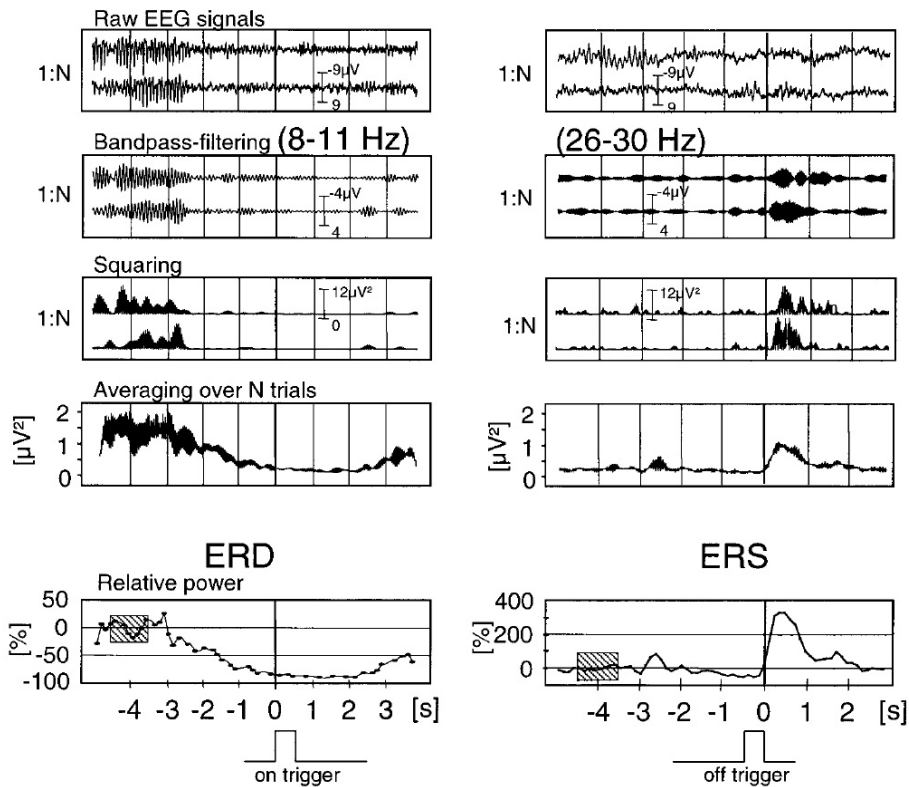


Figure 1.6: The procedure of observing ERD/ERS. [14]

time-frequency map. This analysis contains more information, we use this technique much in this thesis. The ERD/ERS issue is very important in a motor-related BCI. As for this thesis, we are trying to enhance the ERD to ERS ratio in a wrist imagery movement task. The details will be described in section 3.4.3.

## 1.4 Brain-computer Interface

Over the past few decades, the EEG has been used mainly for evaluation of neurological disorders in the clinic and for the investigation of brain functions. Until recently, researchers found it possible to translate some specific EEG to commands. That is, people can communicate with others or control devices directly by their brain activity, without using any normal pathways of the peripheral nerves. This communication and control technique



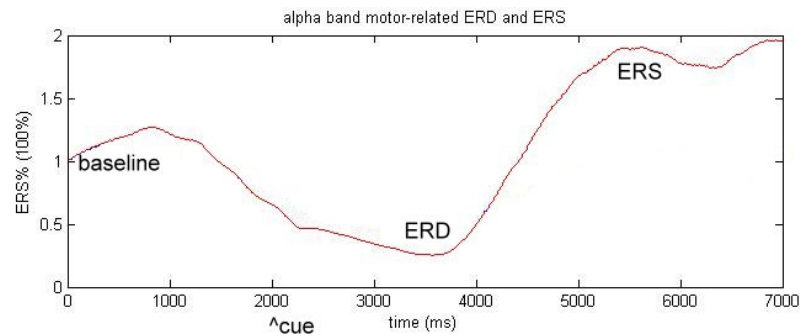


Figure 1.7: Movement related alpha ERD and ERS. The cue point was a visual cue indicating the subject to perform hand movement. When the movement is proceeding, there is an ERD, and when the movement terminates, there is an ERS.

was then called Brain-computer Interface.

A Brain-computer interface is defined as a communication system that does not depend on the brain's normal output pathways of peripheral nerves and muscles. Among the methods to measure electrical activity, MEG and EEG are more suitable for a BCI system because they can give the instantaneous continuous recording of brain activity. And EEG is even more suitable because of the following advantages: the devices to measure EEG are more portable and cheaper, and we don't have to be in a shielding room when measuring EEG. Although the EEG signal is having low spatial resolution compared to the others. Almost all BCI researches are using EEG signal nowadays.

A general BCI flowchart is as figure 1.8 shows. The BCI system goes through the data acquisition, then some signal processing, followed by a command translation, in the end output commands to communicate with others or to control cursors or devices. The details of a BCI system will be described in the next chapter.

## 1.5 Thesis Overview

Chapter 2 provides the overview of BCI systems, including the basic components and key-issues. We also introduce some present-day BCIs here. The methods used in our BCI will be introduced in Chapter 3. We mainly want to design and test an optimal spatial filter to filter the data. With the noise suppressed and features enhanced, we can obtain

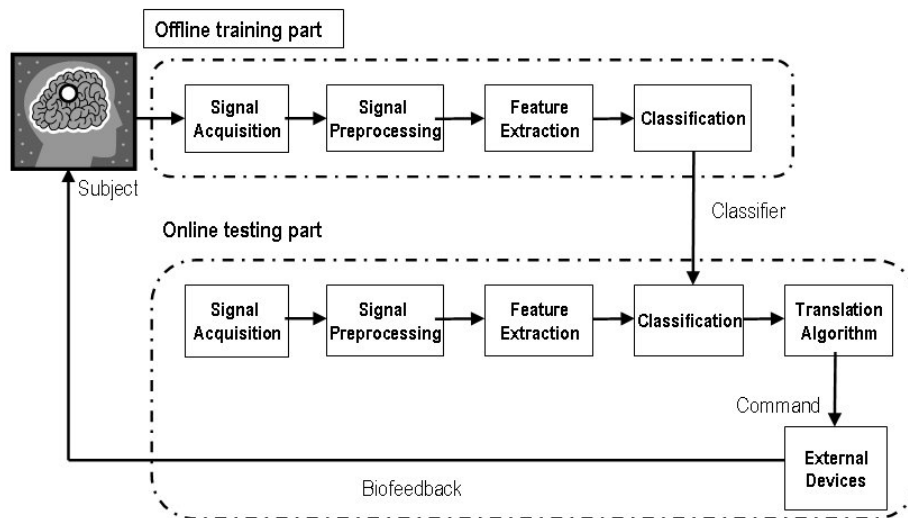


Figure 1.8: The general flowchart of a BCI.

significant data for further classification. Chapter 4 provides the experiment results of our designed offline experiments. We show the analysis results of the spatial filter along with some further performance evaluation results. In chapter 5, we show the experiment results of online feedback sessions and give some brief discussion. In chapter 6 and 7 we give this thesis some conclusion and detailed discussions, including the stability of our spatial filter, the feedback issue, the adaptation issue, and the future works.

## **Chapter 2**

# **Overview of Brain-computer Interface**



In this chapter we will give an overview to BCI systems. We first introduce some categories of BCI systems, then we briefly introduce some present-day BCIs. Next we list and explain some basic components and nowadays key-issues in a BCI system. In the end of this chapter we provide the thesis scope.

## 2.1 Categories of Brain-computer Interface systems

### Synchronous and asynchronous systems

In a synchronous BCI, the user is notified to perform a mental activity when a specific external cue is shown. That means this kind of system operates in a cue-based mode and has the information about the onset of the mental activity in advance. The analyses and classification of the brain signals in the system is limited to the predefined fixed time period. Besides, the system is active only during the predefined period as well. BCI systems based on evoked potentials and ERPs belong to this category, such as P300 [2], SCP [8]. Besides ERPs, the BCI developed in Graz [15] that analyzed the spontaneous EEG are also synchronous BCIs.

The BCI that a user can intend a mental activity whenever he wishes to perform such mental activity is an asynchronous BCI. In the asynchronous BCI, the brain signals are analyzed and classified continuously. We have to not only classify from the redefined mental tasks but also discriminate events from noise and nonevents such as resting or idling states. Such a BCI system is more flexible and attractive to be utilized in practice. Besides the above advantages, it also offer a rapider response time than synchronous ones. However, the classification in an asynchronous BCI system is not accurate enough today.

## 2.2 Basic Components in BCIs

### Signal pre-processing

The goal of the stage is to enhance the signal-to-noise ratio. Typical procedures include amplification, filtering, possible artifact removal. For the filtering, the bandpass filtering is usually applied. In addition, a notch filter is also used to suppress the 60 Hz power line

interference. As for the artifact removal, almost all BCIs rule out the signals if the EOG or EMG is detected to be used or over a predefined threshold.

### **Feature Extraction**

In this stage, certain features are extracted from the preprocessed signals. ERP, ERD/ERS and brain rhythms are typically used features in a BCI system. Besides the above features, various feature extraction methods have been studied to extract more discriminative features, such as Common Spatial filter, continuous wavelet transform, autoregress model(AR) or adaptive autoregress(AAR) model, power spectrum. All the above methods can be found in BCI competition 2003 papers.

### **Classification**

The features extracted from feature extraction are fed to train a classifier. Many classification methods have been proposed in pattern recognition field. The classifier in a BCI can be anything from a simple linear model to a complex nonlinear or a machine learning models. In general, the BCI has two phases training phase and testing phase. The training phase consists of a repetitive process of cue-based mental tasks to train a classifier. In the testing phase, we use the classifier built in the training phase to recognize different mental tasks.

### **Command Translation**

The goal of this step is to translate the classification output in previous step to an operator command. The command can be, e.g., a letter in a spelling system or a movement of a course on the user's screen or nothing to be performed when the classification is "resting" or "idle". The design of translation algorithm and device control depends on what applications the BCI want to provide with.

### **Biofeedback**

A feedback which make the user more easily adaptive to the system is a very important component for a BCI system. A feedback can indicate how well the asked mental activity

was recognized by the system. When the system gives the feedback to a user, he will create a biofeedback which is the process that the user receives information about his biological state.

By Biofeedback, the user can monitor his physiological states, shape his brain electrical behavior, and voluntary modification of his EEG response. Today, nearly all BCI systems provide a feedback to users.

## 2.3 Present-day BCI systems

Here we introduce some present-day BCI systems, we mainly introduce two kinds of BCI systems, the ERP-based BCI and the motor-imagery based BCI.

### 2.3.1 ERP-based BCI

The details about ERP is described in section 2.3.1, because the ERP is evoked by the external events, this kind of BCI usually depends on the gaze of the user. We can always detect the ERP as long as we have enough trials. This kind of BCI has its advantages like the short training time and high accuracy. The drawbacks are the transition rate may be slow and the users may habituate to the system and lower the performance. Here we introduce two main ERP-based BCI, the P300-based and SSVEP-based BCI.

#### P300-based BCI

Farwell proposed a spelling BCI system based on P300 ERP [3]. In this system, users are gazing at a 6x6 matrix on the screen. In the matrix there are letters, numbers, and symbols. When the system starts, it flashes each row and column in the matrix with random sequence. The user is asked to focus his attention on the symbol he wants to select and count the number of time that this symbol is flashed. This is an oddball paradigm and there will be an evoked P300 when the selected symbol is flashed. With enough trials, the system can predict the selected symbol by detecting the P300 response. That's the concept of this BCI system.

### SSVEP-based BCI

The SSVEP is Steady-state Visual Evoked Potential. It is a response to a visual stimulus with a specific high frequency. The EEG signal power will increase at the specific stimulus frequency. Therefore with some different frequency stimulus on the screen we can detect which one has the user's gaze. There are lots of BCI application using SSVEP, such as Lalor [9], his team developed a game to balance a character on the screen using SSVEP.

#### 2.3.2 Motor-imagery based BCI

Compared to the ERP-based BCI, the motor-imagery based BCI is more independent. This kind of BCI basically no need to depend on the user's gaze. The motor-imagery is a spontaneously induced EEG signal. Therefore this kind of BCI is more difficult to develop since the imagery and the concentration of each user may be different. This kind of BCI has its advantages like high transition rate, and users may improve the performance through constant training. The drawbacks are, the training time is longer than a ERP-based BCI, and the user's concentration is very important. Here we introduce the Graz group. [13]. The leader of this group is Dr. Gert Pfurtscheller. This group is in the Graz University of Technology in Austria. The Graz BCI is one of the most successful BCI using motor-imagery tasks. The development is mostly based on the detection of the ERD and ERS pattern in a motor-imagery task. Actually the concept of ERD and ERS was proposed by Pfurtscheller [14]. In their works there are lots of research about different movement that causes different kind of ERD and ERS. They've found some movement related ERD and ERS [14] such as:

- pre-movement alpha ERD

Different voluntary movement will induce an alpha band (8-12Hz) ERD in the corresponding area of motor cortex. The study shows that this alpha ERD starts 1 or 2 seconds before the movement onset. The alpha band power keeps decreasing until the movement terminates. Then there is a ERS after the execution of movement. This ERS is seen as a recovery of the pre-movement ERD.

- post-movement beta ERS

Same as the alpha ERD described above. The study shows that there exists a beta band (16-32 Hz) ERS after the movement terminates.

Today this group is focus on the feature extraction of the ERD and ERS pattern and the classification of different movement imagery. The intend to classify left/right hand movement imagery, foot movement imagery, or tongue movement imagery. They use spatial filter as Common Spatial Pattern (CSP) or morlet wavelet transforms to extract the features. Furthermore they try Support Vector Machine (SVM) or Linear Discriminant Analysis (LDA) in the classification part.

## 2.4 Limitations

Although the BCI systems we introduced above looks well, there are still some limitations in present-day BCI systems. Here we list some normal difficulties when doing researches on BCI systems.

### Habituation

In a ERP-based BCI 2.3.1, we use the evoked potential from the subjects to develop a BCI system. For the evoked potential is not controlled by our own will, we may get used to the BCI system and that affects the performance. Take P300-based BCI for example, if a user use the BCI system day after day, year after year, he/she may habituates to the BCI, and his/her P300 response therefore reduces. This kind of habituation restricts the BCI systems that relays on the ERP responses.

### Noise

As we mentioned before, the EEG signal is poor on the Signal-to-noise ratio. The artifact noise is always a big problem in analysing EEG signals. Eye blinking, eye movements, the heart beating, any possible single small movement causes artifact noises to the EEG signal. Furthermore, not only an artifact causes noises. The interference from the environment, the power line, or the devices, they are also contaminating the EEG signal. In a BCI system, we detect the spontaneous EEG signals or the evoked potential. Both are



very small changes and can be easily affected by these noises. In addition to the artifacts and interference, a distraction of the user also causes noises to the EEG signal. As a human being is very complicated, every little cognitive task has its own response on the EEG signal. We can't be sure that every user of the BCI system are always concentrating to the system, one may easily lose concentration and that reduces the performance of a BCI.

### **Fatigue**

Another limitation to BCI systems is the fatigue of the users. As we introduced in the previous section, the ERP-based BCI keeps giving stimulus to the users and detect their responses. These stimuli may be some quickly changed pictures or flashing, and these fatigue a user easily. Even if in a motor-imagery based BCI, the users may get tired easily because of the continuous concentrate on the imagenary.

## **2.5 Key-issues in BCI systems**

Here we list some key-issues in BCI systems. The future researches on BCI systems may be mostly about these difficult issues.

### **Noise Reduction**

As we mentioned in the previous section, the noise is a limitation to the EEG analyses and BCI systems. How to reduce the noise and the non-interested signals is an issue. Today there are some practical methods to reduce the noises, such as EOG rejection, bandpass filtering, Independent component analysis (ICA), or Laplacian spatial filtering. In this thesis, we designed a spatial filter to filter the data. The filtered data suppresses the non-target noises and enhanced the motor-imagery induced responses. We'll discuss this in the next chapter.

### **Features**

How to find significant features from the EEG signal is an important issue. People have been trying with many methods to extract significant features from the raw EEG data. In

this work, we use the designed spatial filter to suppress the noise and enhance the power change in the signal. Like the CSP [11] method, we can view our spatial filtering approach as feature extraction.

### **Adaptation**

There are two adaptation issues in a BCI system. The first is the users should adapt themselves to the system, that is, self-training of the users. The second is, the BCI system should adapt itself to the users, that is a machine learning issue. Both adaptation issues are important, and these two issues work totally different. If we are trying to self-training a user, we should lower the variability of the BCI system, or the users may not be able to get himself trained well because the feedback keeps changing. The training of the users is still a difficult question. In this work, we use a online visual feedback experiment to observe this user adaptation issue, we'll discuss this in chapter 5.



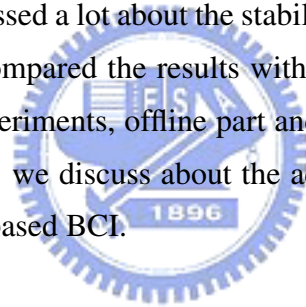
### **Biofeedback**

As we mentioned before, the biofeedback is a important component in the BCI system. Nearly all BCI systems need a biofeedback to the users. This issue is about how the biofeedback affects the users, and how to design useful biofeedback. The design of different biofeedback may result in different mental work and stimulus, which influences on the signal. Not all the influence of a biofeedback is beneficial, it may be harmful as well. For example, the biofeedback stimulus may distract the user from the task. The flase classification may frustrate the user and affect the performance. In a cursor control system, if the cursor moves too fast, the user may get nervous and therefore lower the performance. How to design a useful biofeedback to improve the learning between users and computers is very important. We should always evaluate the effect of biofeedback when designing online systems. In this work we design some visual feedback, this will be discussed in chapter 5.

## 2.6 Thesis scope

In this thesis, we proposed a Brain-computer Interface using motor-imagery EEG. The main idea is to apply a spatial filter to the 32 channel data, and after the linear combination of these channels we can have a more significant signal with a hidden meaning of cortical activity. The idea of the spatial filter is from the source localization problem. We use a technique called Maximum Contrast Beamformer, which was originally used in the source localization problem. The concept of Beamformer technique is using the minimum variance and unit gain constrain to find a spatial filter that suppresses the nontarget noises. And as for Maximum contrast Beamformer, its concept is to use a maximum contrast between control and active state to optimize the dipole orientation in the Beamformer technique. Then the filtered result should be 1. nontarget noises suppressed, 2. maximum contrast between two states, 3. with the meaning of the source signal.

In this thesis, we discussed a lot about the stability and effectiveness of the spatial filter, including the. Also we compared the results with the well-known CSP spatial filter. We performed two part of experiments, offline part and online feedback part, to test the using of this filter. Furthermore, we discuss about the adaptation issue and the visual feedback issue in a motor-imagery based BCI.



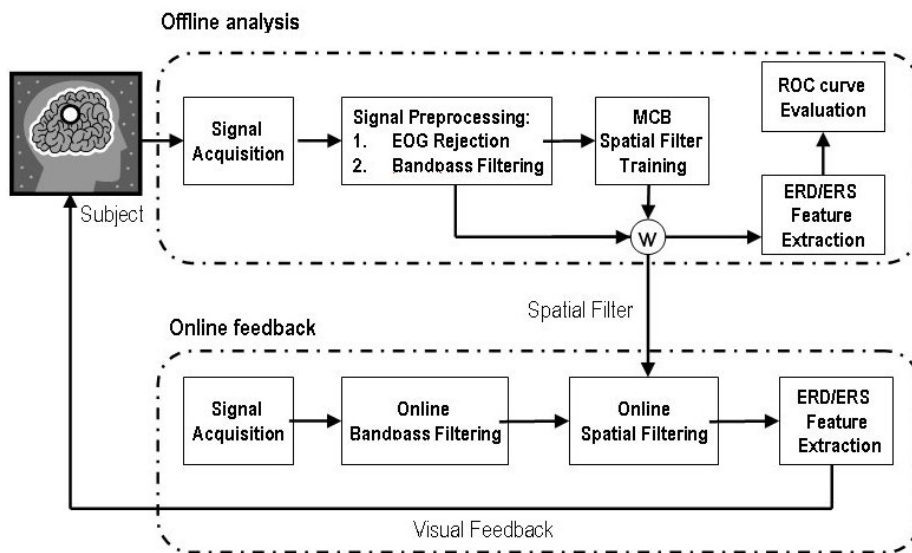


Figure 2.1: Flowchart of proposed BCI.

## **Chapter 3**

# **Cortical activity analysis for BCI**



In this chapter we will introduce the techniques we use in this work. First we introduce the main ideas. Then we introduce the details about the techniques we use, including the data preprocessing methods, the morlet wavelet transform, the spatial filter Maximum Contrast Beamforming (MCB), and the Receiver Operation Curve (ROC) evaluation technique [17] for online simulation. In the end of this chapter we give the idea of our offline and online experiments design. The experiment results will be provided in the next two chapters.

### 3.1 Main ideas

We know from the previous researches that when a human performs movement tasks, there exists pre-movement alpha band ERD and followed by a post-movement beta band ERS [12] in the EEG recorded from the motor cortex. Different part of the body movement represents this phenomenon in different area in the motor cortex. Furthermore, not only real movement tasks have this response, but also imagery movements [12]. In this work, first we use this as the most important prior knowledge.

In this work, we mainly try to use a spatial filter to suppress the noise and enhance the power change in the EEG signal recorded in a motor-imagery task. This spatial filter is based on Maximum-Contrast Beamformer technique, which was used in the source localization issue. By several advantages of this spatial filter, we can obtain more significant signal and do the further classification.

After we construct the spatial filter, we test a lot on it to evaluate the effectiveness. Furthermore, we study the feedback issue and the adaptation issue from an online experiment.

### 3.2 Data acquisition and preprocessing

#### acquisition

The data is acquired under 1000Hz sampling rate. We use a 32 channel EEG cap in which the electrodes are placed under international 10-20 rule.

### preprocessing

We mainly use two preprocessing techniques here: The artifact removal and the band-pass filtering.

As we mentioned in the previous chapter, the artifact exists in EEG signal and significantly affects the data. We apply the EOG rejection to avoid eye blinking and eye movement in our data. The EOG rejection is to simply decide a threshold. Then we remove any single trial that has a single sample exceeds the threshold. This procedure may reduce the trial number used in the further analysis. The threshold we use here is 100  $\mu\text{V}$ .

As for the bandpass filtering, we use a Butterworth bandpass filter to filter the data. We filter the data from 5Hz to 30Hz, this will eliminate the 60Hz power line effect on the signal, the low frequency heart beating (ECG), and the high frequency EMG effects. Before the further analysis on the spatial filter construction, we filter the data from 8Hz to 12Hz (alpha band). This is due to the observation result from our experiments.

## 3.3 Time-frequency analysis

In this work we use morlet wavelet transform to observe the time-frequency map (TF-map). Wavelet transform is a signal processing technique. Similar to Fourier transform analysis which consists of breaking up a signal into sine waves of various frequencies, wavelet transform is of breaking up a signal into shifted and scaled versions of the original wavelet. There are many kinds of wavelets, and Morlet wavelet is one of the well-known wavelets in time-frequency analysis. The basis of Morlet wavelet is

$$Wf(f, t) = Ae^{\left(\frac{-t^2}{2\sigma_t^2}\right)} e^{(2i\pi ft)} \quad (3.1)$$

After the morlet wavelet transform we can obtain the coefficients in a time-frequency map, as figure 3.1 shows. The X-axle is time and the Y-axle is frequency, the color in the map represents the coefficients. The red color means large coefficients and the blue color means the small coefficients. We can observe the map and see which frequency band has explicit power change and at which time point. Take figure 3.1 for example, this is the TF-map of a left wrist imagery movement task. The visual cue indicating the imagery is

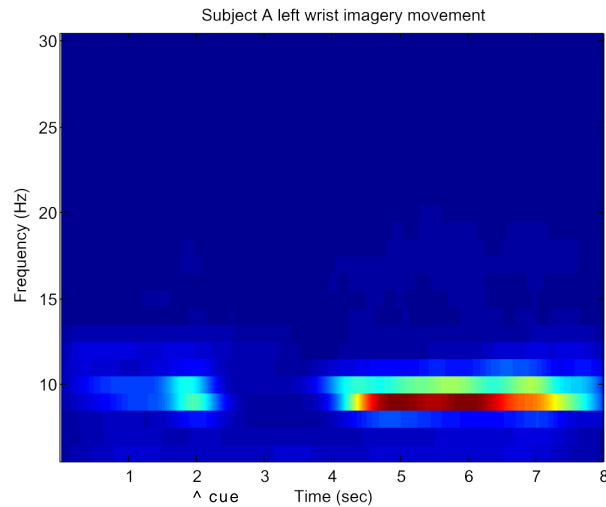


Figure 3.1: Example of a Time-frequency map. This is a left wrist motor imagery task, and the visual cue is given at 2 second. We use the data recorded from C4 channel in this analysis.

at 2 second. Here we can see that about 3 seconds after the visual cue, there is a power increasing lasting for 2 seconds in the frequency band around 10Hz. That is the post-movement Event-related Synchronization (ERS).

In this work we largely use the TF-map analysis to decide the ERS period and ERD period in the motor-imagery task. More precisely, we use the data recorded from the C4 channel, which is known as the channel related to left hand movement tasks, and apply the morlet wavelet transform to plot the TF-map. Then from observing the map we can select the time period of control state and active state. Then we use this information for the spatial filter weighting calculation.

### 3.4 Spatial filtering

In this section we introduce the concept of the spatial filtering technique. We mainly focus on the introduction of Beamforming technique we applied.



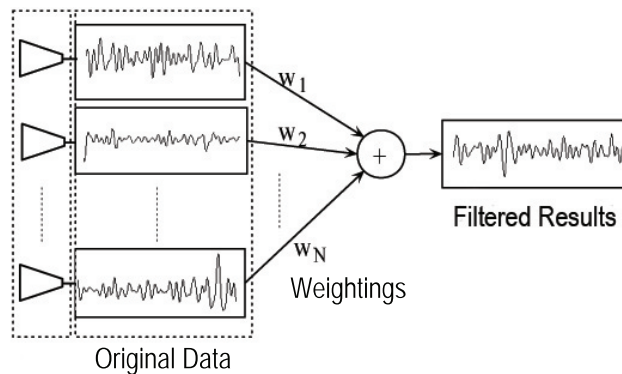


Figure 3.2: The concept of spatial filtering. Each channel has its weighting, and the linear combination of the data acquired from whole channels is called spatial filtering.

### 3.4.1 Introduction

The spatial filtering technique is as figure 3.2 shows. The EEG cap has lots of electrodes, in our case, 32 channels. If we give every channel a weighting then multiply the data recorded from each channel by the corresponding weighting and add them together, we can obtain a new signal. This is for short the linear combination of the channels. We call this technique as spatial filtering, and the weighting vector is called the spatial filter. One main objective in the spatial filtering technique is to enhance the signal-to-noise ratio (SNR). Obviously the difficulty in this technique is the method in finding the weightings. There are many simple spatial filters, next we introduce the spatial filtering technique we use, the Maximum-Contrast Beamformer (MCB), which is developed in our laboratory.

### 3.4.2 Beamforming technique

Beamforming is a technique to localize the source signal with some measured data that is produced by the source signal. It is widely used in many fields like radar, sonar, and astronomical telescope systems. Take radar for example, if we want to localize the airplane by its voice signal measured by radar, we put some radar array on the ground and apply this Beamforming technique on the measured data.

In the EEG source localization problem, we can use this technique as well. We use the EEG electrodes to measure the data as the radar does in the above case. By applying

this technique we can give the EEG source localization problem a solution. Here in this work we are not solving the localization problem. We use the spatial filter trained in this technique to filter the raw data we have. Then the filtered data will be more significant due to the constraints in this technique. In the following sections we introduce the main points in this technique. Then we introduce the use of the developed method Maximum-Contrast Beamformer (MCB).

### Forward Model

The forward model is the information of the measured data sensors and the source signal. Given a source, we can calculate the scalp potential induced by the source. In the Beamforming technique we need the forward model information. In this work we use the overlapping sphere technique to construct the forward model. The idea of the method is using multi-shell geometry rather than BEM model to estimate the overlapping sphere. By assuming that human head had  $m$  layers and estimate the surface potential by the second kind Fredholm integral. We use digitizer to measure the surface of realistic head and then calculate the overlapping sphere for each EEG sensor by minimizing the difference between the multi-shell sphere and realistic head. The details for constructing the spatial filter using the forward model will be introduced in next chapter.

### Beamforming

Beamforming [1] [7] is a method to localize the signal source during array signal processing. It was developed in middle of 20th century and widely used in different field such as sonar, radar and astronomical telescope array systems. The aim of this method is to calculate a set of weighting of the physical channels, called beamforming coefficients. By linearly combine the recording signals with corresponding coefficients, we can create a virtual sensor at a specified position with a specified dipole orientation. In , Van Veen [18] proposed a linearly constrained minimum variance (LCMV) method for implementation of beamforming on EEG/MEG. First we briefly introduce the data model used in the beamforming technique and the simple concept of beamforming. Then the detail of calculating the dipole orientation in this technique will be provided.

Under the system of  $N$  channel EEG sensors, the measured surface potential  $\mathbf{m}$  at an instant time can be regarded as an  $N \times 1$  vector expressed by

$$\mathbf{m} = \mathbf{G}(\mathbf{r})\mathbf{q} = \mathbf{G}(\mathbf{r})\frac{\mathbf{q}}{\|\mathbf{q}\|}\|\mathbf{q}\| = \mathbf{l}(\mathbf{r}; \mathbf{q})\|\mathbf{q}\| \quad (3.2)$$

where  $\mathbf{G}(\mathbf{r})$  is the gain matrix calculated by forward model and  $\mathbf{l}(\mathbf{r}; \mathbf{q})$  is the leadfield. More precisely, leadfield means the measurement with the dipole source located at  $\mathbf{r}$  with dipole moment  $\mathbf{q}$  which composed by dipole orientation  $\frac{\mathbf{q}}{\|\mathbf{q}\|}$  and dipole strength  $\|\mathbf{q}\|$ . Furthermore, when there are  $k$  dipole sources at an instant time, we model the noise as an  $N \times 1$  vector  $\mathbf{n}$ . The measured data can be rewritten as

$$\mathbf{m} = \sum_{i=1}^k \mathbf{l}(\mathbf{r}_i; \mathbf{q}_i)\|\mathbf{q}_i\| + \mathbf{n} \quad (3.3)$$

where  $\mathbf{q}_i$  ( $i = 1, 2, \dots, k$ ) is the  $i$ th dipole moment.

Notice that the equation above represents the measurement at an instant time. In time domain, bio-medical signal is often modeled as a random signal and thus we take temporal information into consideration and we use first and second order statistics to describe the dipole as

$$\bar{\mathbf{q}}_i = E\{\mathbf{q}_i\} \quad (3.4)$$

$$c_{q_i} = E\{[q_i - \bar{q}_i][q_i - \bar{q}_i]^T\}, \quad (3.5)$$

respectively, where  $E$  stands for expectation. Furthermore, the mean and covariance matrix of the measurement are

$$\bar{\mathbf{m}} = E\{\mathbf{m}\} = \sum_{i=1}^k \mathbf{l}(\mathbf{r}_i; \mathbf{q}_i)\bar{q}_i \quad (3.6)$$

$$\mathbf{C} = E\{\|\mathbf{m}(\mathbf{q}_i) - \bar{\mathbf{m}}\|\|\mathbf{m}(\mathbf{q}_i) - \bar{\mathbf{m}}\|^T\} = \sum_{i=1}^L \mathbf{l}(\mathbf{r}_i; \mathbf{q}_i)c_{q_i}\mathbf{l}^T(\mathbf{r}_i; \mathbf{q}_i) + \mathbf{C}_n \quad (3.7)$$

respectively, where  $\mathbf{C}_n$  is the covariance of the noise under an assumption of zero mean. Practically,  $\mathbf{C}$  is calculated by using recorded EEG signals.

$$\mathbf{C} = \frac{1}{N-1} \mathbf{M}_{MDF} \mathbf{M}_{MDF}^T \quad (3.8)$$

where  $T$  is the sampling number and  $\mathbf{M}$  is an  $N \times T$  matrix which represents the recorded EEG signals. The subscript "MDF" denotes Mean-Deviation Form which each element is substituted by the mean of row of original matrix (i.e. averaged potential of each sensor).

As mentioned in previous section, beamforming is designed to reconstruct the source activation by linearly combine the recordings from each EEG sensor. The idea can be written as

$$y = \mathbf{w}^T(\mathbf{r}_0; \mathbf{q}_0) \mathbf{m} \quad (3.9)$$

where  $y$  is the reconstructed moment with dipole location  $r_0$  and dipole orientation  $\frac{\mathbf{q}}{\|\mathbf{q}\|}$ , and  $\mathbf{w}^T(\mathbf{r}_0; \mathbf{q}_0)$  is an  $N \times 1$  vector which denotes the spatial filter. By LCMV, there are two constraints in finding  $w$ . The first one is **linearly constrained**:

$$\mathbf{w}^T(\mathbf{r}_0; \mathbf{q}_0) \mathbf{l}(\mathbf{r}_0; \mathbf{q}_0) = 1 \quad (3.10)$$

which extracts the target source ( $\mathbf{r} = \mathbf{r}_0$  and  $\mathbf{q} = \mathbf{q}_0$ ) and suppresses other sources ( $\mathbf{r} \neq \mathbf{r}_0$  and  $\mathbf{q} \neq \mathbf{q}_0$ ). This constraint is also called *unit gain constraint* because after filtering the predicted potential, we would get the original source. The second idea of LCMV is **minimum variance**:

$$\min_{\mathbf{w}(\mathbf{r}_0; \mathbf{q}_0)} c_y \text{ s.t. } \mathbf{w}^T(\mathbf{r}_0; \mathbf{q}_0) \mathbf{l}(\mathbf{r}_0; \mathbf{q}_0) = 1 \quad (3.11)$$

where  $c_y$  is the variance of the estimated signal. The reason to minimize the variance of the filtered signal is that if forward model is exactly correct and without noise, then

$$y_0 = \mathbf{w}^T(\mathbf{r}_0; \mathbf{q}_0) \mathbf{m} = \mathbf{w}^T(\mathbf{r}_0; \mathbf{q}_0) \mathbf{l}(\mathbf{r}_0; \mathbf{q}_0) \mathbf{q}_0 = 1 \times \mathbf{q}_0 = \mathbf{q}_0 \quad (3.12)$$

where  $\mathbf{q}_0$  is the true source moment at the target position. The details in solving the filter  $\mathbf{w}$  are in [18] and the equation is:

$$\mathbf{w} = (\mathbf{C} + \alpha \mathbf{I})^{-1} \mathbf{l} (\mathbf{l}^T (\mathbf{C} + \alpha \mathbf{I})^{-1} \mathbf{l})^{-1} = \frac{(\mathbf{C} + \alpha \mathbf{I})^{-1} \mathbf{l}}{\mathbf{l}^T (\mathbf{C} + \alpha \mathbf{I})^{-1} \mathbf{l}} \quad (3.13)$$

where  $\alpha$  is a regularization parameter,  $\mathbf{C}$  is the covariance matrix explained in previous section and  $\mathbf{I}$  is the identity matrix. Here we omit  $(\mathbf{r}_0; \mathbf{q}_0)$  for simplicity.

### 3.4.3 Maximum Contrast Beamformer

However, there is still one question - "How do we know the dipole orientation?" . In accordance with this question, LCMV decomposes the orientation solution space with 3 orthogonal basis in 3D space. Robinson and Vrba proposes *synthetic aperture magnetometry (SAM)* method to search the orientation such that the resultant value of z-deviate is maximum. However, we use a new method to calculate the optimal dipole orientation analytically. In this section we provide the details in this method and explain how we use it in designing a filter for a BCI system.

The decision of dipole orientation is an important issue in beamforming techniques. A correct dipole orientation can successfully suppress the undesired noise. The idea of MCB is finding the optimal dipole orientation by maximizing the ratio of active state and control state. In the beginning, recall the definition we gave before. The leadfield  $\mathbf{l} = \mathbf{G}(\mathbf{r}) \frac{\mathbf{q}}{\|\mathbf{q}\|}$  can be rewritten as  $\mathbf{l} = \mathbf{G}\mathbf{j}$  and substitute it into Eq 3.13 we have

$$\mathbf{w} = \frac{(\mathbf{C} + \alpha\mathbf{I})^{-1}\mathbf{l}}{\mathbf{l}^T(\mathbf{C} + \alpha\mathbf{I})^{-1}\mathbf{l}} = \frac{(\mathbf{C} + \alpha\mathbf{I})^{-1}\mathbf{G}\mathbf{j}}{\mathbf{j}^T\mathbf{G}^T(\mathbf{C} + \alpha\mathbf{I})^{-1}\mathbf{G}\mathbf{j}} \doteq \frac{\mathbf{A}\mathbf{j}}{\mathbf{j}^T\mathbf{B}\mathbf{j}} \quad (3.14)$$

where  $\mathbf{A} = (\mathbf{C} + \alpha\mathbf{I})^{-1}\mathbf{G}$  and  $\mathbf{B} = \mathbf{G}^T(\mathbf{C} + \alpha\mathbf{I})^{-1}\mathbf{G}$ . Notice that the dipole orientation  $\mathbf{j}$  could be extracted. In the idea of MCB, we maximize the ratio between active and control state by using F statistic for the criterion in deciding the ratio. The formula is

$$\mathbf{F} = \frac{\mathbf{w}^T \mathbf{C}_a \mathbf{w}}{\mathbf{w}^T \mathbf{C}_c \mathbf{w}} \quad (3.15)$$

After substituting Eq 3.14 into Eq 3.15, the formula can be translated as:

$$\tilde{\mathbf{j}} = \arg \max_{\mathbf{j}} \frac{(\frac{\mathbf{A}\mathbf{j}}{\mathbf{j}^T\mathbf{B}\mathbf{j}})^T \mathbf{C}_a (\frac{\mathbf{A}\mathbf{j}}{\mathbf{j}^T\mathbf{B}\mathbf{j}})}{(\frac{\mathbf{A}\mathbf{j}}{\mathbf{j}^T\mathbf{B}\mathbf{j}})^T \mathbf{C}_c (\frac{\mathbf{A}\mathbf{j}}{\mathbf{j}^T\mathbf{B}\mathbf{j}})} = \max_{\mathbf{j}} \frac{\mathbf{j}^T \mathbf{A}^T \mathbf{C}_a \mathbf{A} \mathbf{j}}{\mathbf{j}^T \mathbf{A}^T \mathbf{C}_c \mathbf{A} \mathbf{j}} \doteq \max_{\mathbf{j}} \frac{\mathbf{j}^T \mathbf{P} \mathbf{j}}{\mathbf{j}^T \mathbf{Q} \mathbf{j}} \quad (3.16)$$

where  $\mathbf{P} = \mathbf{A}^T \mathbf{C}_a \mathbf{A}$  and  $\mathbf{Q} = \mathbf{A}^T \mathbf{C}_c \mathbf{A}$ . Now we can know that it is a traditional optimization problem in solving  $\mathbf{j}$  and the solution is the eigenvector with respect to the maximum

eigenvalue of matrix  $\mathbf{Q}^{-1}\mathbf{P}$ . Therefore, we determined the source orientation with deterministic computational steps.

The inter-subject variability is always a critical problem in EEG signal analysis. In the same motor-related task, two different subjects may have the ERD and ERS in different frequency range. Therefore, before we start to train this spatial filter, there are few things we should decide first.

1. *Frequency band* : The frequency band of the subject should be decided first, we use the morlet wavelet transform to observe the frequency band as we mentioned before. From the time-frequency map we can decide not only the frequency band, but also the time period of active and control state.
2. *Selection of active/control state* : Here we select the time period of the two state. Our experience is to select a 0.5 second range time period. We select the ERD period as the control state and the ERS as the active state. We discuss about the selection issue in chapter 5.
3. *Dipole position* : As mentioned before, the dipole position is used to calculate the forward model. First we observe the MRI and decide the position which is representing the hand area in the motor cortex. After more experiments have done, we find we can roughly decide the position and still get good results.
4. *Optimal regularization parameter* : The regularization parameter refers to the  $\alpha$  in Eq 3.13. A value of  $10^{-7}$  is applied in the general cases.
5. *Feature extraction* : After the signal was filtered by the spatial filter, we extract the feature for classification by calculating the ERD/ERS curve of the signal. We take the 1 second period before the visual cue as the baseline and continue the calculation according to the step described in section 1.3.3

All the results of experiments and the details for deciding the parameters above will be shown in next chapter.

## 3.5 Thresholding

After the spatial filtering, the ERD and ERS should be enhanced and the noise should be suppressed. Here we use a simple scheme illustrated by the paper proposed in 2004 [17] to evaluate the performance of the spatial filter if we apply it online. That is the sample-by-sample ROC curve analysis.

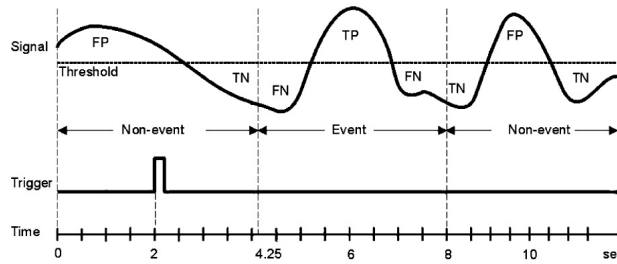


Figure 3.3: The ROC curve analysis. [17]

### 3.5.1 ROC curve analysis

In a ROC curve figure, the x-axle is the False-Positive Rate (FPR) and the y-axle is the True-Positive Rate (TPR). The TPR and FPR are defined as

$$TPR = \frac{TP}{TP + FN}, FPR = \frac{FP}{TN + FP} \quad (3.17)$$

and the term TP, FN, FP, and TN indicate True-Positive, False-Negative, False-Positive, and True-Negative. These terms can be seen in figure 3.3. Where the TP means the threshold classifier classify this sample point as positive (there is a motor movement), and it's a correct classification. TN means the classifier classify this point as negative (this is resting state), and it's a correct. While FN and FP are the incorrect cases, respectively indicates type I error and type II error in statistics.





# Chapter 4

# Experiments



In this chapter we show the experiment results in our work. We mainly designed two part of experiments, the offline training session and the online feedback session. In the following, first we introduce the detail of the experiment setup, including the experiment paradigm, the data acquisition, the equipment setup, and the subjects. Second we show the details of the data preprocessing and the signal processing procedures. Then we provide the experiment results of all subjects and give some brief observation.

In every dataset, we mainly provide three kinds of analysis result. That is the Time-frequency analysis results, the spatial filtering results, and the ROC curve analysis results. We give figures along with tables to help understanding the results.

Further discussions and conclusions will be provided in the next chapter.

## 4.1 Offline analysis

### 4.1.1 Experiment setup

#### Experiment paradigm

The experiment paradigm is as figure 4.1. At the beginning of each trial, a fixation cross appears on the screen indicating the subject to focus on it. The cross lasts for two seconds, after then a warning tone sounds and a left/right arrow appears on the screen, lasting for 1.5 seconds. The arrows are cues indicating the subjects to perform either a left or right wrist lifting imagery task. The subjects are told to perform the task after he/she sees the arrow disappears. Each trial ends 8 seconds after the cross appears. Because the subjects' habit to the regularity might lead to implicit results, we apply a jittering in the paradigm to avoid so. That is, there is a randomly given 2 to 4 second interval between each trial.

There are two sessions in one experiment. In the first session, subjects are asked to perform left or right wrist lifting real movement. And in the second session, the tasks are left or right wrist lifting imagery movement. Each session goes for twenty minutes, and between two sessions there is a few minute break to avoid fatigue of the subjects. Because of the random interval between trials, the numbers of trials in each session are not always the same. But there are at least 50 trials in each task.



## Subjects

We invited five subjects in this experiment, including four males and one female, all aged 22-24. Each subject participates three to six experiments. We asked these subjects to participate one experiment about every ten days. The different number of experiment times are according to his/her performance of the results. Finally, subject A participates 5 experiments, subject B participates 3 experiments, subject C participates 5 experiments, and both subject D and subject E participate 3 experiments. In the above five, the raw data of subject E is somehow too bad to analyse. We have too few trials left after the pre-processing, so in the following results we skip the subject E. Therefore, we'll show totally 16 experiments, including 16 real movement sessions and 16 imagery movement sessions.

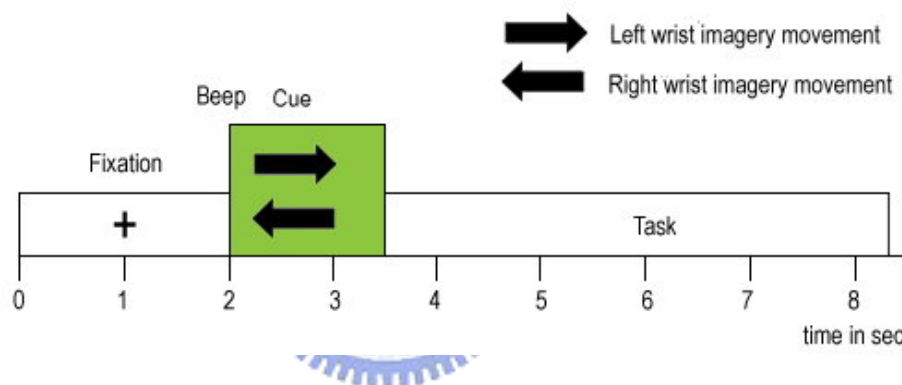


Figure 4.1: Experiment paradigm. This figure shows the experiment paradigm of wrist lifting. The time line indicates what the screen shows in every second.

## Equipment setup

We prepared two computers and an 32-channel EEG cap connecting to an amplifier. The subject is asked to wear the EEG cap and sit on a comfortable chair, putting his/her hands on the table and keep them relax. There is a 17" LCD monitor set in front of the the subject, and the screen shows the visual cue described in section 4.1.1. This paradigm is controlled by computer A. The timing of each cue is sent from computer A through a parallel port to computer B, which is connected to the amplifier and records the data along with the cue points.

The data acquisition is under 1000Hz sampling rate. We start the experiment after the impedance of all 32 channels are below 3k ohm.

After an experiment is done, we use a digitizer to record the exact 3D electrode positions. This information is needed as head model. We use it to calculate the forward model described in section 3.4.2 used in the MCB spatial filtering method in section 3.4.3.

### Data pre-processing

After the data is recored, we apply some preprocessing:

- 1 EOG rejection. When the eye blinks, it brings out EOG and strongly affects the data, especially the data recorded from the frontal channels. The detail of EOG rejection was described in section 3.2. Here we use 100 microvolt as the threshold and reject any trial that has data points exceeding this threshold.
- 2 Bandpass filtering. We apply a 5-30 Hz bandpass filter to the data. On one hand to avoid low frequency heartbeat artifacts, and on the other to avoid the 60 Hz power line effects and high frequency noises.

### 4.1.2 Data analysis

Here we show the analyses we did after the data was pre-processed.

#### Time-frequency analysis

First we do some basic analyses to the data. Mainly because we want to make sure the data is fine before we do any further analysis. The main analysis here is Time-Frequency analysis using morlet wavelet transform, as we described in section 3.3. We need to observe some parameters to train the MCB spatial filter described in section 3.4.3, such as control/active state time period selection.

#### Spatial filter training

After the basic analysis we select two time periods as control state and active state. We then use this information along with the forward model to train a MCB spatial filter for

each data. The filtered result compared to the original C4 channel data is shown in the next section. Also we analyse the filter weighting and plot it as topography map in the next chapter.

### ROC curve analysis

The ROC curve analysis is used to simulate the offline data as a online recorded data. The procedure is described in section 3.5. After the training of the MCB spatial filter is done, we apply the filter to the data and compare the ROC curve between raw C4 channel data and the filtered data. From the two ROC curves we can observe the best TPR and FPR that a simple threshold can give. We then compare it to see if this scheme works.

### 4.1.3 Experiment results

#### Subject A

- Experiment 1

The TF-map is shown in figure 4.2. The filtered result compared with the C4 channel data is shown in figure 4.3.

- Experiment 2

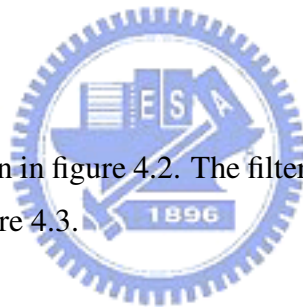
The TF-map is shown in figure 4.4. The filtered result compared with the C4 channel data is shown in figure 4.5.

- Experiment 3

The TF-map is shown in figure 4.6. The filtered result compared with the C4 channel data is shown in figure 4.7.

- Experiment 4

The TF-map is shown in figure 4.8. The filtered result compared with the C4 channel data is shown in figure 4.9.



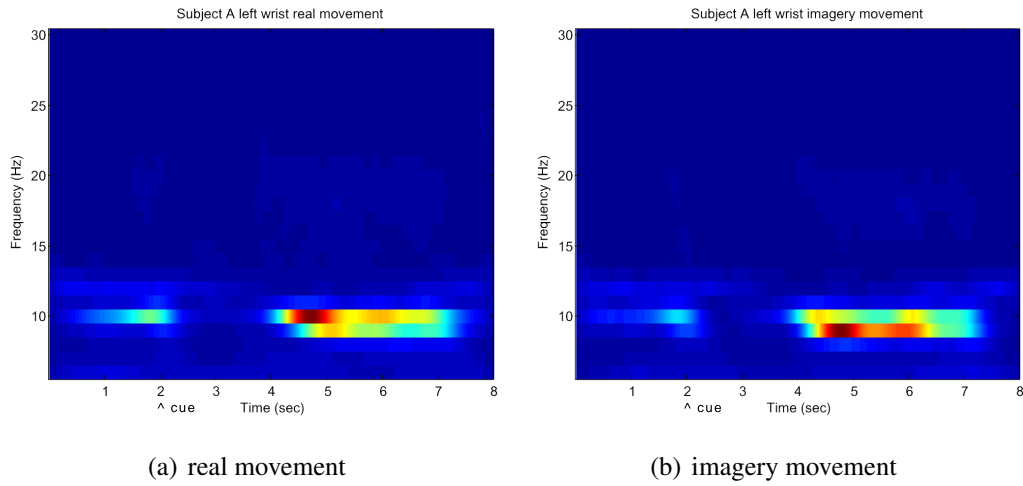


Figure 4.2: The Time-Frequency map of Subject A. The frequency ranges from 6 to 30 Hz, and the timeline is an eight-second trial. The visual cue indicating the motor movement is at 2 second. The left figure is the real movement session and the right figure is the imagery movement session.

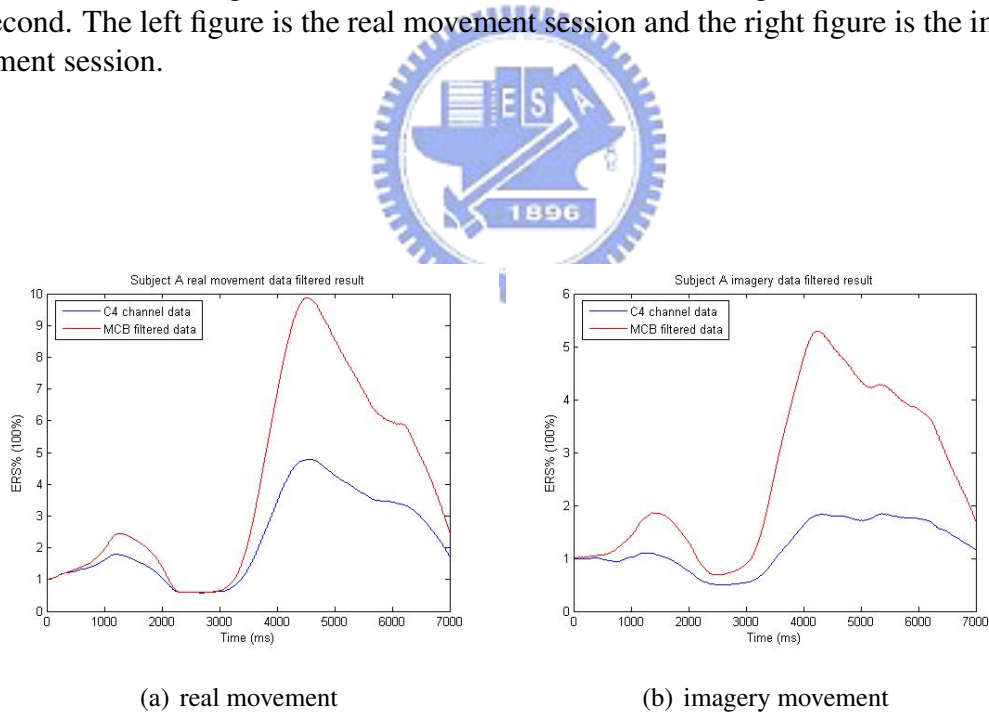


Figure 4.3: The ERD/ERS curve of Experiment 1 of subject A, the visual cue appears at 2 second. The red line indicates the filtered data and the blue line indicates the original C4 data. The left figure is real movement session and the right one is imagery session

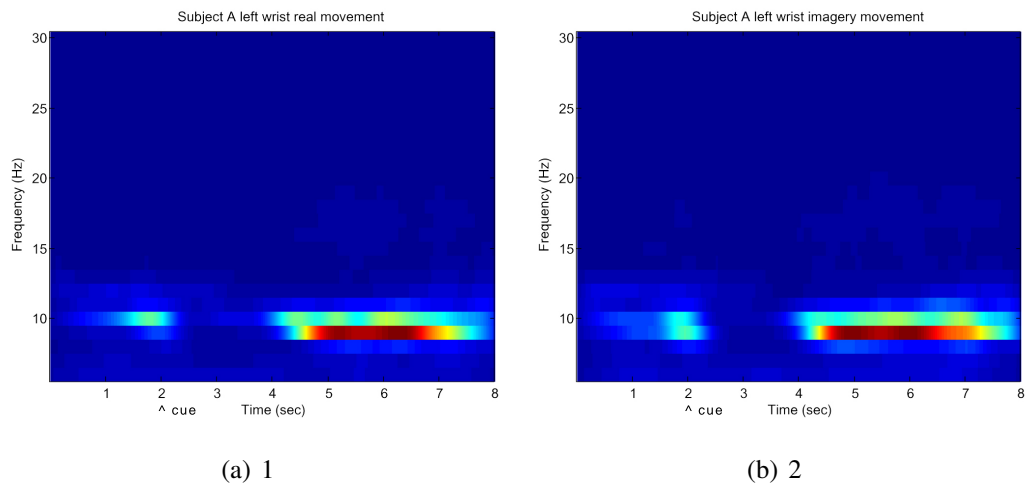


Figure 4.4: The Time-Frequency map of Subject A. The frequency ranges from 6 to 30 Hz, and the timeline is an eight-second trial. The visual cue indicating the motor movement is at 2 second. The left figure is the real movement session and the right figure is the imagery movement session.

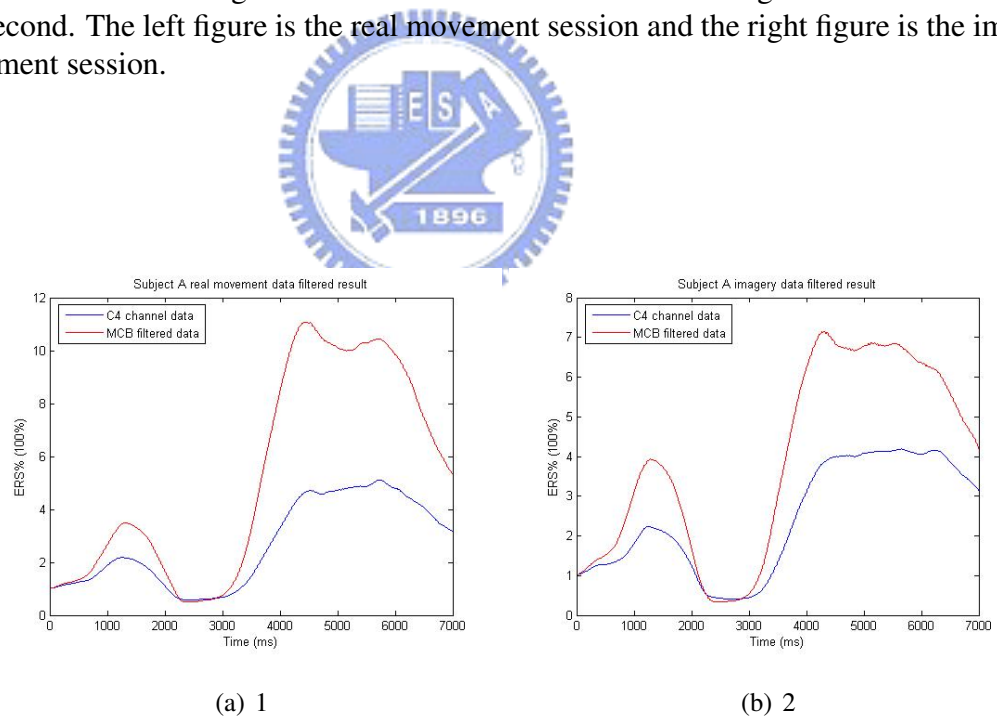


Figure 4.5: The ERD/ERS curve of Experiment 2 of subject A, the visual cue appears at 2 second. The red line indicates the filtered data and the blue line indicates the original C4 data. The left figure is real movement session and the right one is imagery session

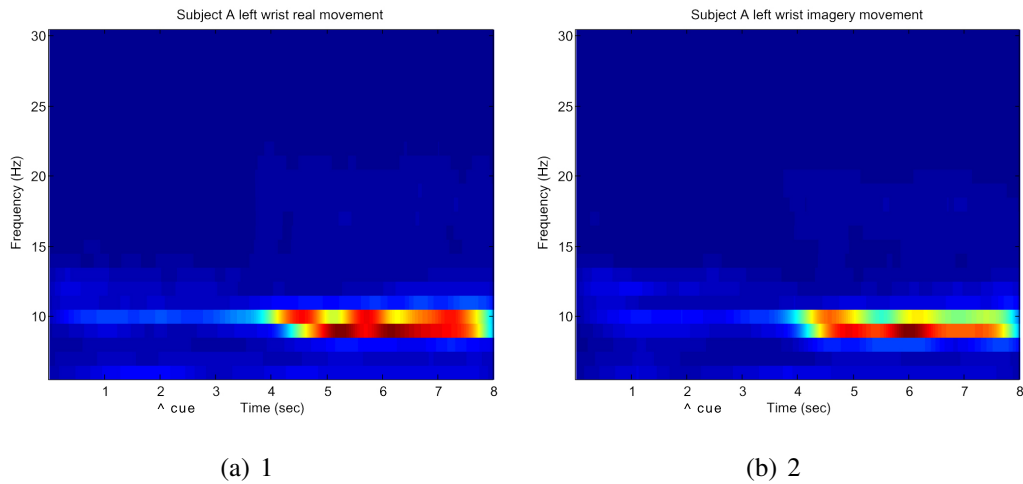


Figure 4.6: The Time-Frequency map of Subject A. The frequency ranges from 6 to 30 Hz, and the timeline is an eight-second trial. The visual cue indicating the motor movement is at 2 second. The left figure is the real movement session and the right figure is the imagery movement session.

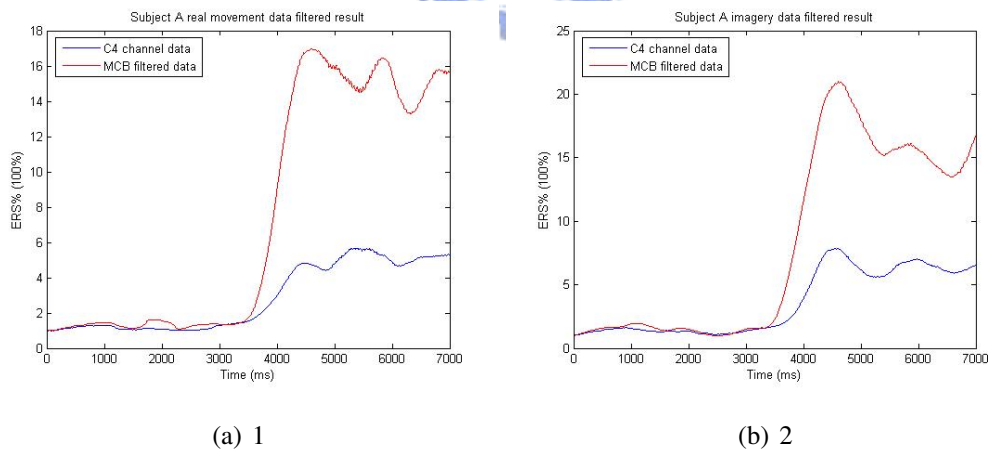


Figure 4.7: The ERD/ERS curve of Experiment 3 of subject A, the visual cue appears at 2 second. The red line indicates the filtered data and the blue line indicates the original C4 data. The left figure is real movement session and the right one is imagery session



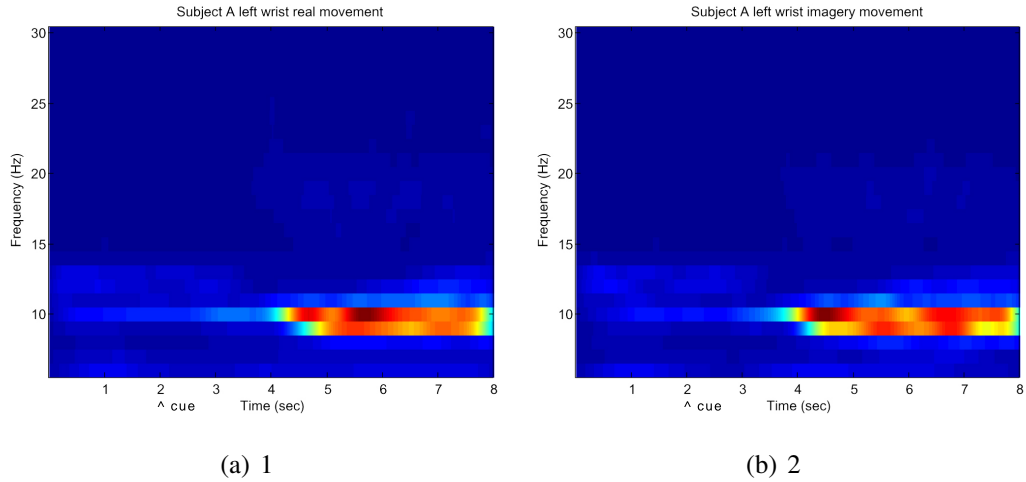


Figure 4.8: The Time-Frequency map of Subject A, Experiment 4. The left figure is the real movement session and the right figure is the imagery movement session.

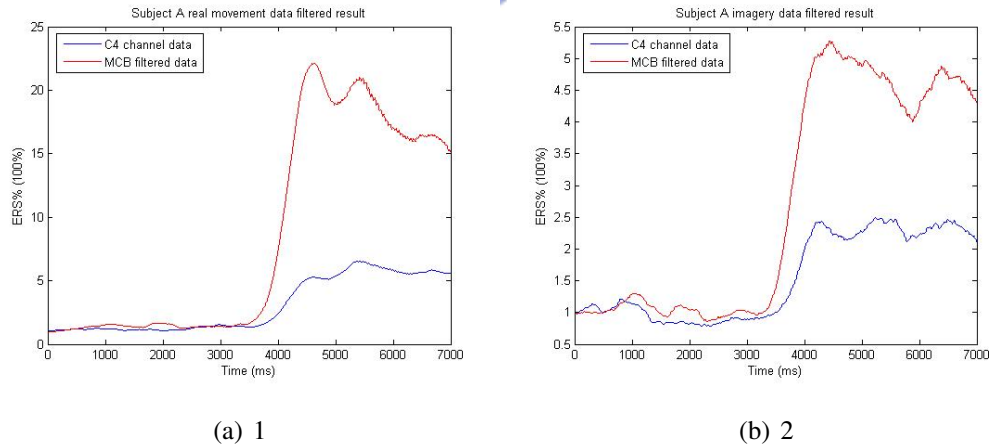


Figure 4.9: The ERD/ERS curve of Experiment 4 of subject A, the visual cue appears at 2 second. The left figure is real movement session and the right one is imagery session

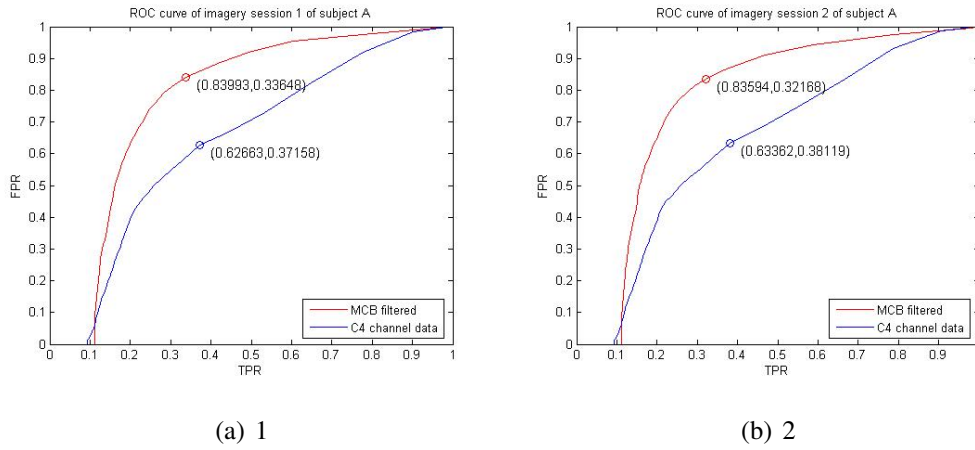


Figure 4.10: ROC curve analysis of Subject A, imagery session 1 and 2. The red line is the ROC curve of the filtered data and the blue line is the ROC curve of the C4 channel data.

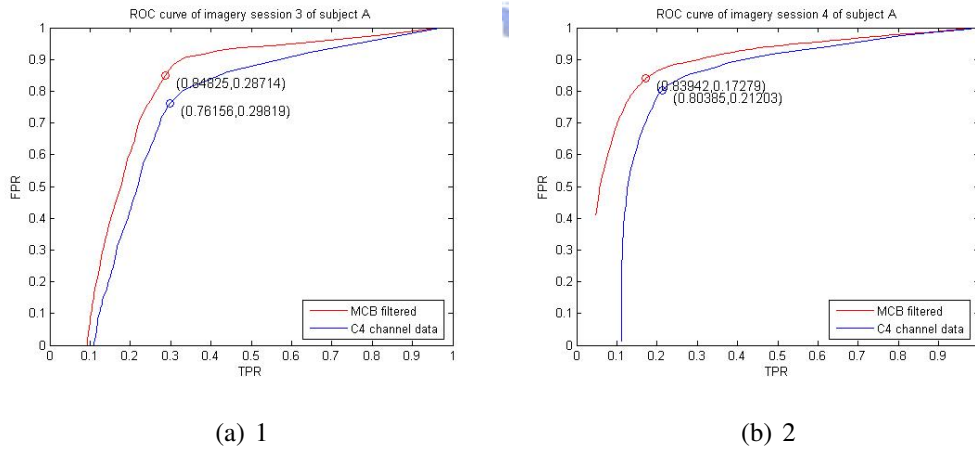


Figure 4.11: ROC curve analysis of Subject A, imagery session 3 and 4. The red line is the ROC curve of the filtered data and the blue line is the ROC curve of the C4 channel data.

subject A left wrist imagery movement

Dataset		ERS%	ERD%	ERS%-ERD%	TPR	FPR
1	C4 channel data	181%	56%	125%	0.62	0.37
	MCB filtered data	369%	74%	295%	0.84	0.33
2	C4 channel data	315%	41%	274%	0.63	0.38
	MCB filtered data	398%	32%	366%	0.83	0.32
3	C4 channel data	447%	89%	358%	0.76	0.29
	MCB filtered data	892%	78%	814%	0.84	0.28
4	C4 channel data	212%	81%	131%	0.80	0.21
	MCB filtered data	408%	89%	319%	0.84	0.17

Table 4.1:

**Subject B**

- Experiment 1

The TF-map is shown in figure 4.12. The filtered result compared with the C4 channel data is shown in figure 4.13.

- Experiment 2

The TF-map is shown in figure 4.14. The filtered result compared with the C4 channel data is shown in figure 4.15.

- Experiment 3

The TF-map is shown in figure 4.16. The filtered result compared with the C4 channel data is shown in figure 4.17.



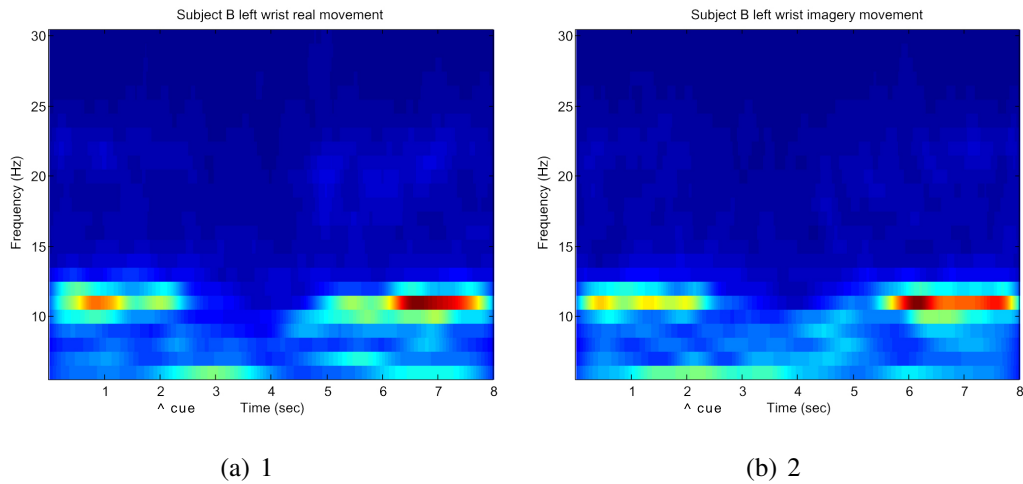


Figure 4.12: The Time-Frequency map of Subject B. The frequency ranges from 6 to 30 Hz, and the timeline is an eight-second trial. The visual cue indicating the motor movement is at 2 second. The left figure is the real movement session and the right figure is the imagery movement session.

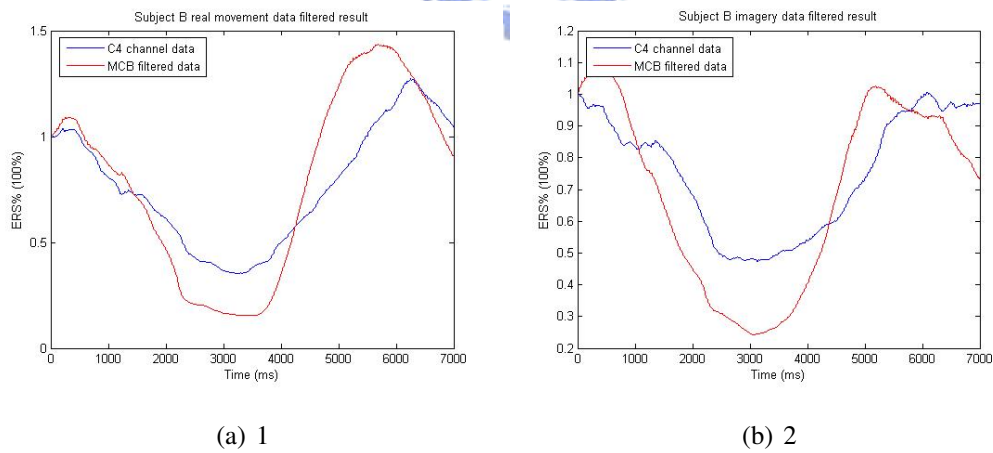


Figure 4.13: The ERD/ERS curve of Experiment 1 of subject B, the visual cue appears at 2 second. The red line indicates the filtered data and the blue line indicates the original C4 data. The left figure is real movement session and the right one is imagery session

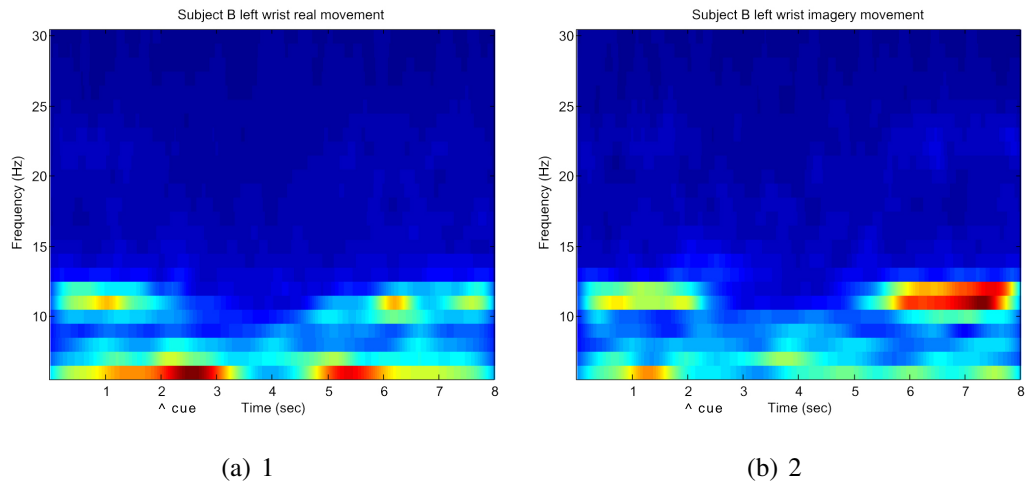


Figure 4.14: The Time-Frequency map of Subject B. The frequency ranges from 6 to 30 Hz, and the timeline is an eight-second trial. The visual cue indicating the motor movement is at 2 second. The left figure is the real movement session and the right figure is the imagery movement session.

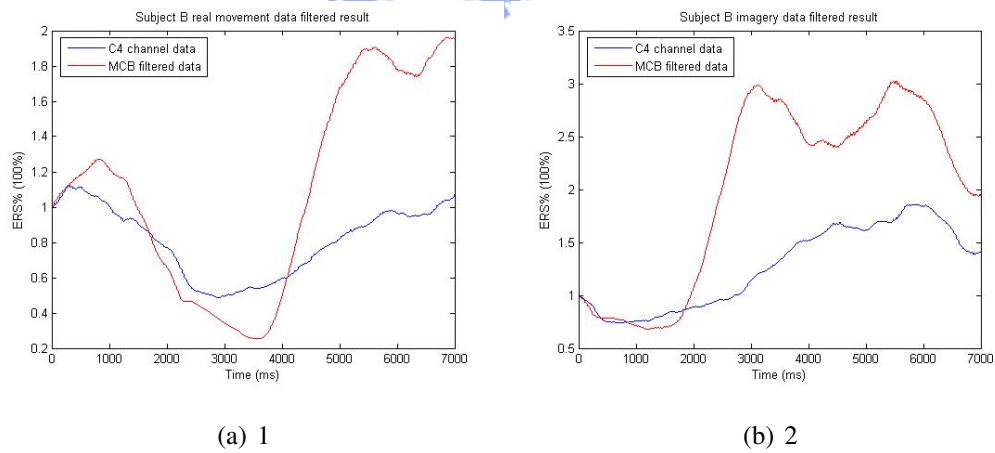


Figure 4.15: The ERD/ERS curve of Experiment 2 of subject B, the visual cue appears at 2 second. The red line indicates the filtered data and the blue line indicates the original C4 data. The left figure is real movement session and the right one is imagery session

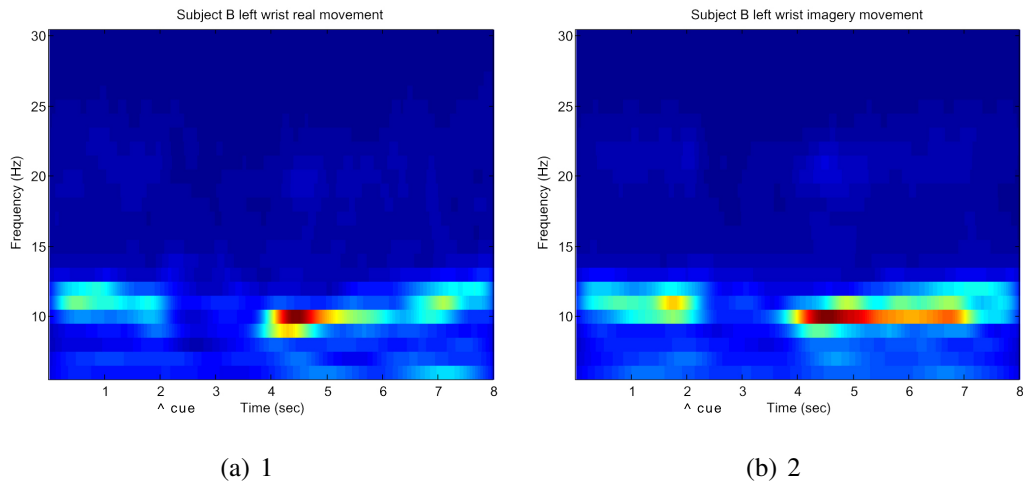


Figure 4.16: The Time-Frequency map of Subject B. The frequency ranges from 6 to 30 Hz, and the timeline is an eight-second trial. The visual cue indicating the motor movement is at 2 second. The left figure is the real movement session and the right figure is the imagery movement session.

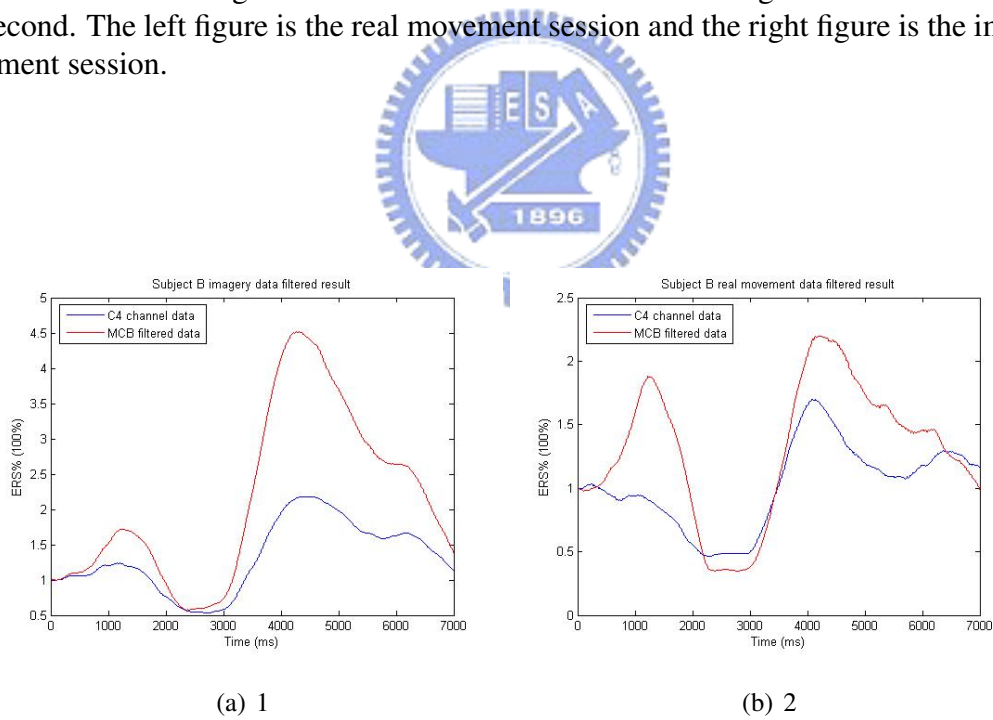


Figure 4.17: The ERD/ERS curve of Experiment 3 of subject B, the visual cue appears at 2 second. The red line indicates the filtered data and the blue line indicates the original C4 data. The left figure is real movement session and the right one is imagery session

**Subject C**

- Experiment 1

The TF-map is shown in figure 4.18. The filtered result compared with the C4 channel data is shown in figure 4.19.

- Experiment 2

The TF-map is shown in figure 4.20. The filtered result compared with the C4 channel data is shown in figure 4.21.

- Experiment 5

The TF-map is shown in figure 4.22. The filtered result compared with the C4 channel data is shown in figure 4.23.







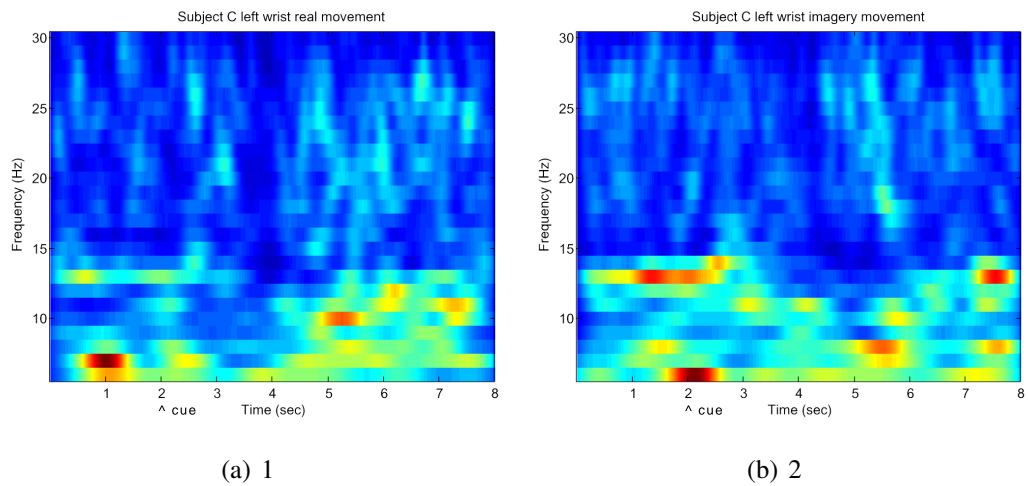


Figure 4.20: The Time-Frequency map of Subject C. The frequency ranges from 6 to 30 Hz, and the timeline is an eight-second trial. The visual cue indicating the motor movement is at 2 second. The left figure is the real movement session and the right figure is the imagery movement session.

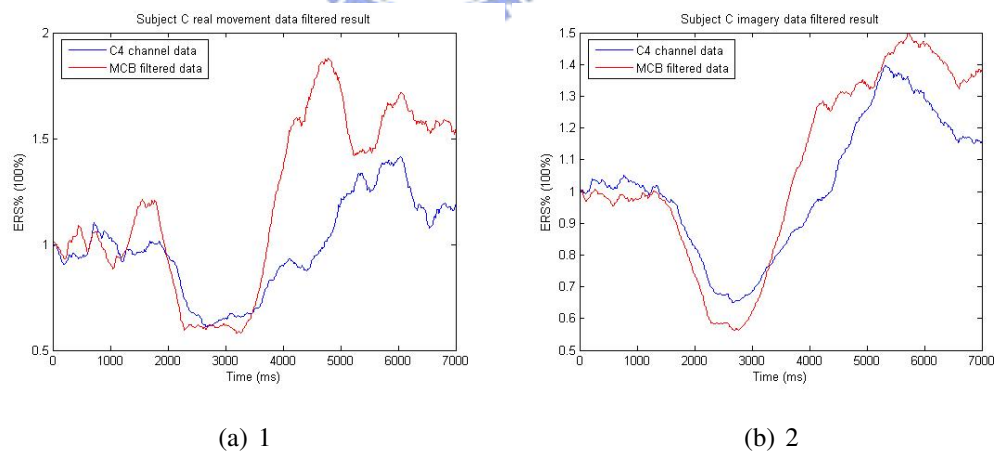


Figure 4.21: The ERD/ERS curve of Experiment 2 of subject C, the visual cue appears at 2 second. The red line indicates the filtered data and the blue line indicates the original C4 data. The left figure is real movement session and the right one is imagery session



**Subject D**

- Experiment 1

The TF-map is shown in figure 4.24. The filtered result compared with the C4 channel data is shown in figure 4.25.

- Experiment 2

The TF-map is shown in figure 4.26. The filtered result compared with the C4 channel data is shown in figure 4.27.





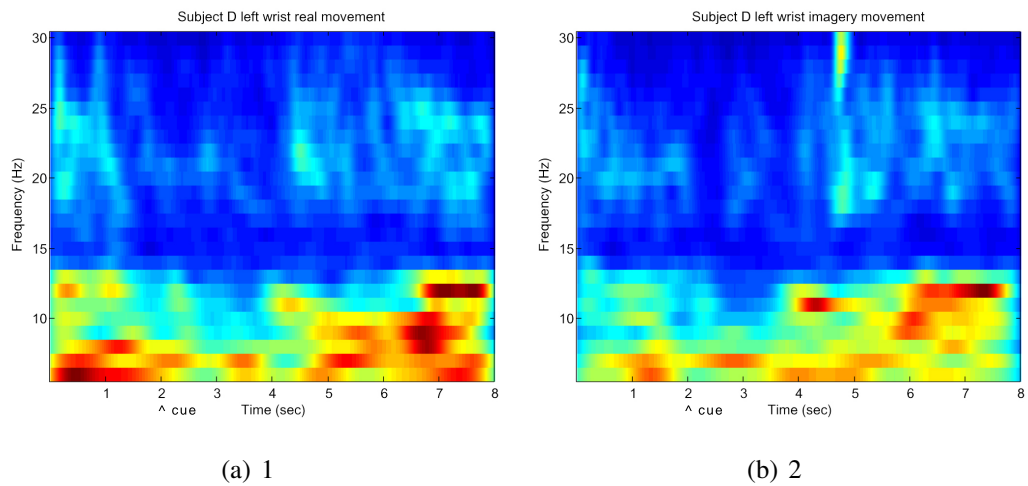


Figure 4.26: The Time-Frequency map of Subject D. The frequency ranges from 6 to 30 Hz, and the timeline is an eight-second trial. The visual cue indicating the motor movement is at 2 second. The left figure is the real movement session and the right figure is the imagery movement session.

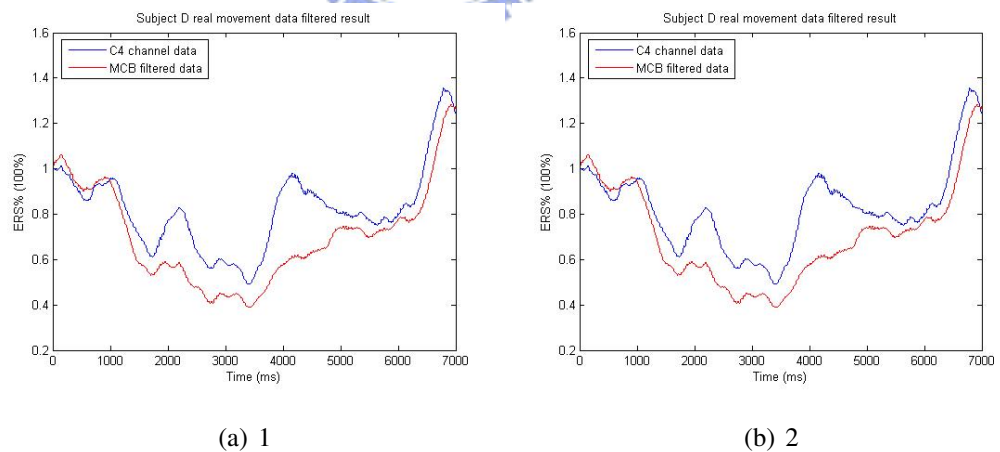


Figure 4.27: The ERD/ERS curve of Experiment 2 of subject D, the visual cue appears at 2 second. The red line indicates the filtered data and the blue line indicates the original C4 data. The left figure is real movement session and the right one is imagery session

## 4.2 Online feedback experiment

In this chapter we show the experiment results of online feedback experiments. First we introduce the experiment setup, including information about session time, trial time, experiment paradigm, data pre-processing, and online processing scheme. Then we show the results of online feedback experiments compared with the offline experiment results. In the end of this chapter we give a brief discussion about our experiment and the results.

### 4.2.1 Experiment setup

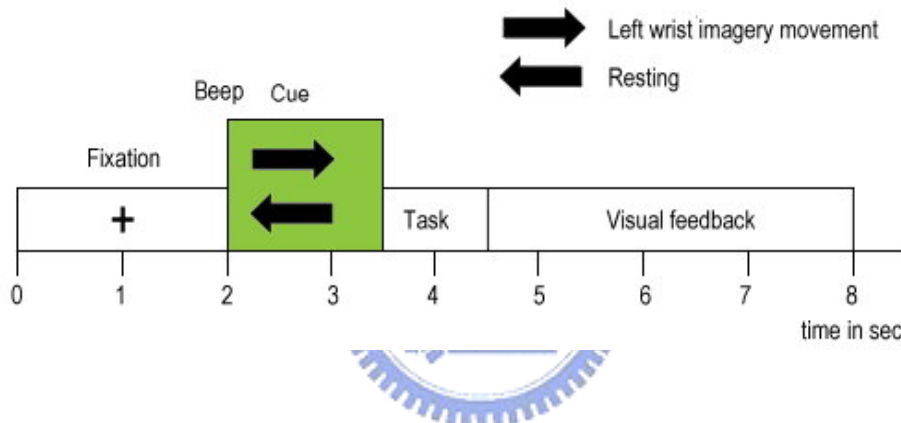


Figure 4.28: Online experiment paradigm design. This figure shows the experiment paradigm of online experiment of wrist imagery movement. The time line indicates what the screen shows in every second. The visual cue appears at 2 second and lasts for 1.5 second. The visual feedback starts at 4.5 second and ends at 8 second.



Figure 4.29: Online experiment visual feedback. The visual feedback is a expanding-contracting bar, indicating the ERS% at the moment.

### Experiment paradigm

The online feedback experiment paradigm is pretty much like the offline one. As figure 4.28 shows, a fixation cross appears in the center of the screen at the beginning of a trial. The cross lasts for 2 seconds and a warning tone sounds, followed with an arrow appearing on the screen, indicating the subject to perform a left wrist imagery movement or to keep resting. The arrow lasts for 3 seconds and a visual feedback starts on the screen. The visual feedback is like figure 4.29. It's a bar extending or contracting as the power changes.

In each experiment, we have two sessions. The first session is just like an offline experiment session described in section 4.1.1. Then we use the data recorded in this session to train a MCB spatial filter, and we apply this spatial filter to online filter the the data in the second session. The second session will give the subjects a visual feedback on the screen according to the online filtered results.

### Subjects

In the online feedback session, we test only one subject. We pick subject A, the one who gets significant results in the offline experiments. We can say he's a well-trained subject. This subject participates 2 online feedback experiments, with a few days interval between them.

### Data processing

In the first session we do the data processing just like we described in the previous chapter. As for the second online feedback session, the data is recorded in 1000Hz sampling rate and is online filtered by an 8-12Hz bandpass filter. We then online apply the spatial filter trained in the first session to the second session.

### Feedback

As for the bio-feedback, we use a expanding-contracting bar indicating the ERS.

## 4.2.2 Experiment results

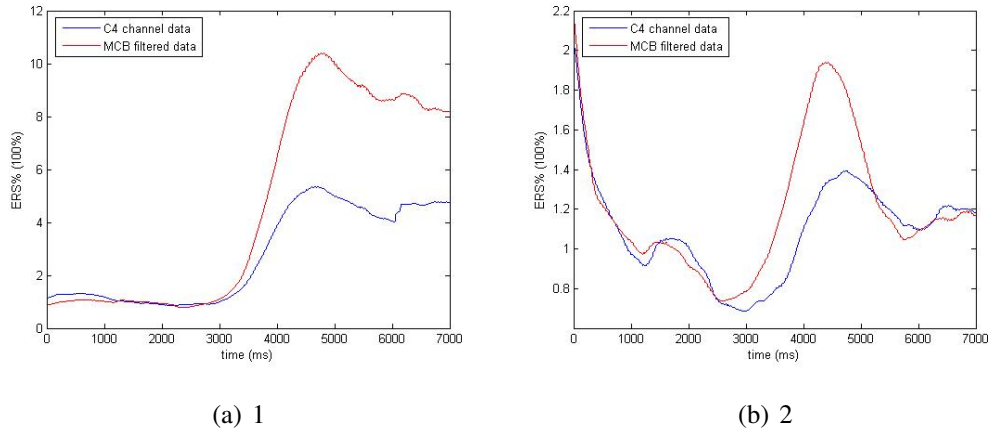


Figure 4.30: The ERD/ERS curve of Experiment 1 of subject A, the visual cue appears at 2 second. The red line indicates the filtered data and the blue line indicates the original C4 data. The left figure is the first session (offline training) and the right one is the second session (online feedback).





## 4.3 Observations

1. The TF-map analysis is useful

From the TF-map we can see that almost every subject, every data has the same result. That is, the alpha band power changing dominants in 5-30Hz. To observe more we can see the alpha band power decreases after the visual cue at 2 second and lasts for about 1 second. Then it's followed by a power increasing and lasts for more than 2 seconds. These ERD and ERS are well-known movement related responses. [14]

2. The imagery movement is similar to real movement

We can observe that the imagery movement datasets and the real movement datasets are having almost the same response. Just the power change of a real movement data is usually more significant than an imagery one.

3. The MCB spatial filter enhances the power change

Comparing C4 channel data and MCB filtered data, we can observe that when the original data is not too bad, the filter works very well in enhancing the ERS to ERD ratio. This performance can be seen especially in the well-trained subject A's datasets, both real movement data and imagery data. Take Subject A, dataset 1, imagery data for example, the ERS to ERD ratio in the original C4 channel data was about 250. After the filtering it changes to about 550. We can say that this spatial filter has its effectiveness.



# Chapter 5

## Discussion



In this chapter we review the brief discussions at the end of experiment results and give some further discussions about the stability and effectiveness of MCB spatial filter, the adaptation issue, the possible causes of the different results between offline and online feedback experiments, and the future works.

## 5.1 Spatial filter

From the experiment results of chapter 4, we believe that the MCB spatial filter has its effectiveness to enhance the ERS to ERD ratio and also suppress the nontarget source signal, that is, noise. And by the enhancement of ERD and ERS in a motor-imagery task, we can make it easier to detect an ERD and ERS pattern using a simple threshold calculated by ROC curve analysis.

But there are still some important issues considering this spatial filter:

1. Does the same spatial filter weighting suit to every subject?
2. Need one subject train his or her own spatial filter every time he or she uses this system?
3. What if we choose a different control state and active state?
4. What is the possible explanation of the filter weighting topography map?
5. How does well-known Common Spatial Pattern (CSP) work here?
6. How many trials do we need to construct a good spatial filter?

We'll discuss these issues.

### 5.1.1 Stability of the spatial filter

In fact, question 1 and question 2 can be combined as the stability issue. Of course the best case is that we construct a subject-independent spatial filter that enhances the ERD to ERS ratio well, but the truth is, the EEG signal is suffering great inter subject variability. Below we compare every subject's most representative spatial filter weighting

by calculation the correlation coefficient. Furthermore, we compare the correlation and filter effectiveness between sessions of a same subject, analysing the variability of the filter between sessions. We split this stability issue to three analyses as below. The correlation coefficient is calculated as

$$R(i, j) = \frac{C(i, j)}{\sqrt{C(i, i)C(j, j)}}, \quad (5.1)$$

where  $C$  denotes the covariance matrix of two weighting vectors. The correlation coefficient is close to 1 when the two weighting vectors are highly correlated, and it's close to 0 when the two vectors are poorly correlated.

### Filter weighting correlation between sessions

In this analysis we want to see if the spatial filter weighting changes a lot in different sessions. We separately calculate each subject's correlation coefficients between different sessions. The result is as table 5.1, table 5.2, table 5.3, and table 5.4 show.

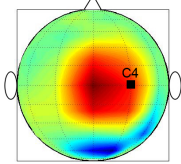
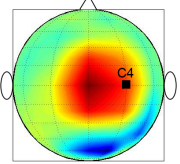
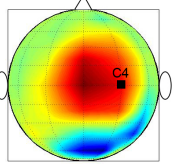
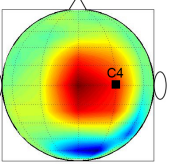
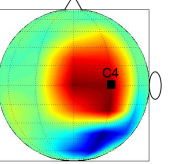
	1	2	3	4	5
					
1	1	0.94	0.93	0.93	0.86
2		1	0.98	0.97	0.85
3			1	0.99	0.91
4				1	0.87
5					1

Table 5.1: Correlation coefficients between different sessions. This table shows the result using wrist real movement datasets of subject A. The number 1 to 5 denotes the session number, and the topography map is viewed from the top of the head.

The results in table 5.1 and table 5.2 show the high correlation between different sessions. This means that although the human brain is complicated and suffering great variability, we can still calculate the similar MCB spatial filter weightings in each session, same

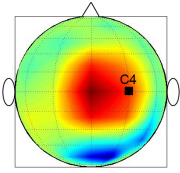
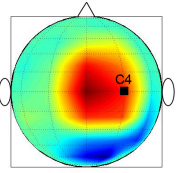
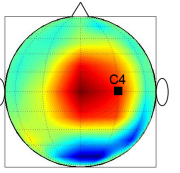
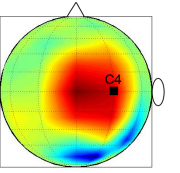
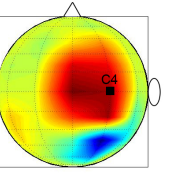
	1	2	3	4	5
					
1	1	0.88	0.84	0.89	0.87
2		1	0.96	0.98	0.86
3			1	0.97	0.92
4				1	0.87
5					1

Table 5.2: Correlation coefficients between different sessions. This table shows the result using wrist imagery movement datasets of subject A. The number 1 to 5 denotes the session number, and the topography map is viewed from the top of the head.

subject. So we may use the stable filter weighting always. From the table, no matter real movement or imagery movement, the correlation between sessions remain high. Another special phenomenon observed here is that the latest session, dataset 5 is the most uncorrelated dataset compared to the others. We may explain this as after a long period of time, the subject's responses of the EEG signal slightly changes.

### Filter weighting correlation between real movement and imagery movement

Here we analyse the correlation between tasks. We take the five datasets of subject A and calculate the correlation coefficient between real movement and imagery movement in each experiment. The result is in table 5.3.

From table 5.3 we can see that the real movement and imagery movement are highly correlated. It means that if a user wants to use the BCI system, he/she may use the data of real movement, which is easier, to train a spatial filter for later imagery tasks. Of course this idea to train the filter using real movement data is unworkable for a motor-disabled patient, but this may work on a normal user. Furthermore, this supports that the real movement and the imagery movement have the similar responses.

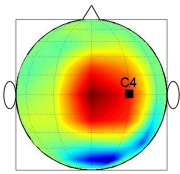
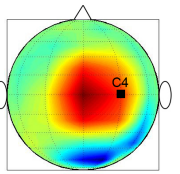
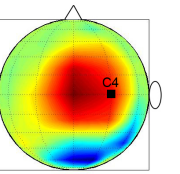
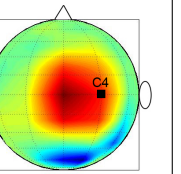
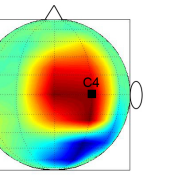
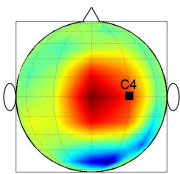
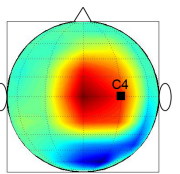
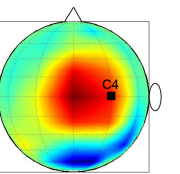
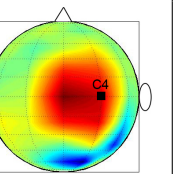
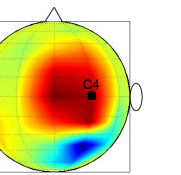
real	1 	2 	3 	4 	5 
img					
corr	0.94	0.99	0.97	0.99	0.94

Table 5.3: Correlation coefficients between different tasks. The first row is the five real movement sessions, the second row is the five imagery sessions, and the third row is the correlation coefficient between the first and second row. Number 1 to 5 denotes the session number, and the topography map is viewed from the top of the head.

### Filter weighting correlation between subjects

In each subject, we select one representative spatial filter weighting and we calculate the correlation coefficients between these weightings. This analysis is to observe if different subjects share the similar spatial filter. If they do, the weightings should be highly correlated, and we may not need to train a new spatial filter every time we have a new subject. We select the representative spatial filter under this rule: the filter that has the weighting vector most highly correlated to the other filter weightings. For instance, we observe table 5.1 and select number 3 spatial filter as it's the most representative one that is highly correlated to the rest four. The result of this analysis is in table 5.4.

From this table we can see that every subject has it's own style of filter weightings. They do not share the filter weightings as the correlation coefficients are poor. This means although each subject has the similar spatial filter trained in different sessions, they should still use the filter trained by their own data.

We conclude the three sub-issues that, every user using a BCI system based on this

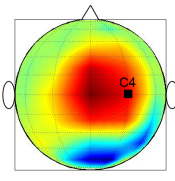
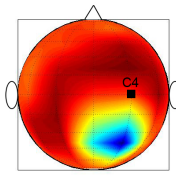
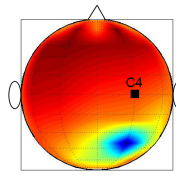
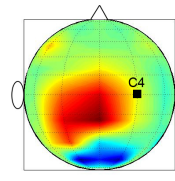
Subjects				
	A	B	C	D
				
A	1	0.34	0.51	0.78
B		1	0.72	0.22
C			1	0.36
D				1

Table 5.4: Correlation coefficients between different subjects. The first row is the five subjects' representative spatial filter weighting topography. Alphabet A to E denotes the subject identity, and the topography map is viewed from the top of the head.

spatial filter that enhance the motor-imagery ERD and ERS should train his or her own spatial filter using his own training data. The subject dependent spatial filter weightings are similar in different sessions every different time we perform the experiment, but after a long period of time it may changes a little bit from the one trained originally. No matter the training data is real movement or imagery movement, the spatial filter should be similar if everything goes fine in the experiments.

### 5.1.2 Different selection of control/active state

In the MCB method, we find a dipole orientation that maximize the variance ratio between active state and control state. In our case we choose the alpha band ERD period as the control state and the ERS period as the active state. How about we choose a totally different period of time as control state or active state? For example, choose the resting period as control state instead. Here we test three kinds of selection on dataset 1 to 4 of Subject A. The three different selection of control/active states are listed below. The results of the 4 real movement datasets are presented in table 5.5, imagery datasets in table table 5.6, and we plot the filtered data compared to the C4 channel data of dataset 1 in figure 5.1.



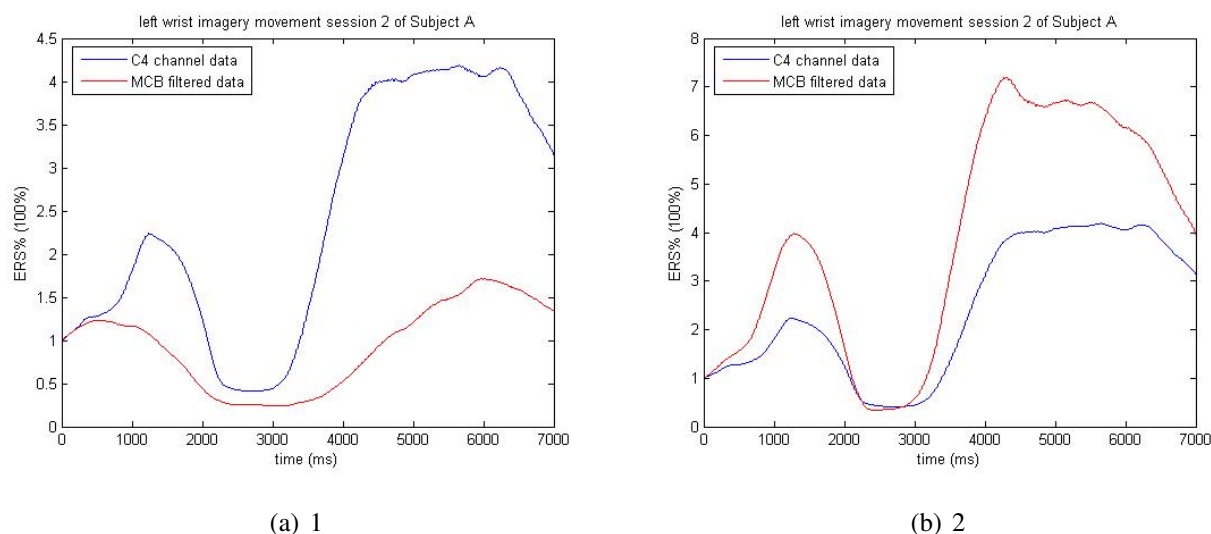


Figure 5.1: Different result when choosing different active/control state. The left figure is using ERD as active state and resting as control state and the right figure is using ERS as active state and resting as control state.



### The resting period as control state and the ERS period as active state

First we test the one that is the most easy selection to guess. We choose the resting period as the control state and the post-movement ERS period as the active state. In our offline experiment paradigm, the resting period should start from about one second before the visual cue appears. As for the ERS period is the same as we selected before, starting about 3 seconds after the visual cue appears. This selection means to suppress the resting period power and to enhance the ERS power increasing. The  $ERS\% - ERD\%$  is used to evaluate the performance of the spatial filter. The plotted result is as figure 5.1 shows and the  $ERS\% - ERD\%$  evaluation is in table 5.5.

From the result we can see that this scheme works as well as the original scheme, just a little bit lower in the  $ERS\% - ERD\%$  evaluation. This is because in subject A's datasets, the power decrease period is usually not very explicit while the post-movement power increase period is phenomenal.

### **The ERD period as control state and the resting period as active state**

Second we select the during-movement ERD period as the control state and the resting period described above as active state. This scheme means we try to find the optimal dipole orientation that maximize the power ratio of resting and ERD, that is, to enhance the ERD%. This scheme should be reasonable since the during-movement alpha ERD is an important phenomenon.

From the result we can see that this scheme poorly enhance the ERD%. The reason should be the same as the previous scheme that the ERD is usually not explicit in this subject. This is depend on the subjects. We can see clear ERD but barely no explicit ERS in subject B.

### **The ERD period as control state and the ERS period as active state**

This scheme is the one described in chapter 4.

Observing the two result tables of subject A we can see that the different selection scheme indeed gives slightly different results, and the results are somehow just like what we expected. But from the comparison figures between subject A and subject B we notice that the best selection scheme of control state and active state is still unknown. Every kind of selection has its reason. We can say that which scheme suits which subject by observing the subject's EEG signal responses, but we should realize that not every subject represents the same. The brainwave is complicated and sometimes varied from subject to subject. We should always observe more in this issue.

### **5.1.3 Comparison between MCB and CSP**

Common Spatial Pattern (CSP) [11] is also called Common Spatial Subspace Decomposition (CSSD). This spatial filter is known for its ability on classifying the motor-imagery tasks. The principle of CSP is to simultaneously diagonalize the two covariance matrices associated with two classes. Then the most discriminative spatial filter can discriminate the two classes. It makes the projected data of one class has the minimum variance and the other data has the maximum variance, therefore discriminate them. The variance of

the sample points on the time domain can be seen as its power. Since the induced power change (the ERD and ERS) is the most phenomenal characteristic in a motor-related task, this filter is used mainly in the motor-related tasks.

The algorithm of CSP [11] is as the following:

1. Calculate the two covariance matrices,  $\Sigma_1$  and  $\Sigma_2$ , of the two classes.

$$\Sigma_1^i = \frac{\mathbf{V}^i \mathbf{V}^{it}}{\text{trace}(\mathbf{V}^i \mathbf{V}^{it})} \quad (5.2)$$

where  $\mathbf{V}^i$  is the raw data of trial  $i$ . The size of  $\mathbf{V}^i$  is  $N \times T$ , presented as  $N$  number of channels and  $T$  samples in time. The  $t$  means transpose.

$$\Sigma_1 = \sum_i \frac{\mathbf{V}^i \mathbf{V}^{iT}}{\text{trace}(\mathbf{V}^i \mathbf{V}^{iT})} \quad (5.3)$$

2. Calculate scatter matrix

$$\Sigma_S = \Sigma_1 + \Sigma_2 \quad (5.4)$$

, which can be diagonalize as

$$\Sigma_S = \mathbf{B}_S \lambda \mathbf{B}_S^t \quad (5.5)$$

Here  $\mathbf{B}_S$  is an  $N \times N$  matrix of normalized eigenvectors, satisfying

$$\mathbf{B}_S \mathbf{B}_S^t = \mathbf{I}_{N \times N} \quad (5.6)$$

$\lambda$  is the diagonal matrix of eigenvalues.

3. Perform the whitening transformation.

$$\mathbf{D}_1 = \mathbf{W} \Sigma_1 \mathbf{W}^t \quad (5.7)$$

$$\mathbf{D}_2 = \mathbf{W} \Sigma_2 \mathbf{W}^t \quad (5.8)$$

with

$$\mathbf{W} = \lambda^{(-1/2)} \mathbf{B}_S^t \quad (5.9)$$

$\mathbf{D}_1$  and  $\mathbf{D}_2$  have the property of  $\mathbf{D}_1 + \mathbf{D}_2 = \mathbf{I}_{N \times N}$  and of sharing the same eigenvectors.

4. Diagonalize  $\mathbf{D}_1$  and  $\mathbf{D}_2$ .

$$\mathbf{D}_1 = \mathbf{U}\Psi_1\mathbf{U}^t; \quad (5.10)$$

$$\mathbf{D}_2 = \mathbf{U}\Psi_2\mathbf{U}^t \quad (5.11)$$

, with the property  $\Psi_1 + \Psi_2 = \mathbf{I}$

5. Calculate the projection matrix  $\mathbf{P}^t$

$$\mathbf{P}^t = \mathbf{U}^t\mathbf{W} \quad (5.12)$$

Apply the projection matrix  $\mathbf{P}^t$  to each  $\mathbf{V}^i$  and then get projected data  $\mathbf{Z}^i$  as

$$\mathbf{Z}^i = \mathbf{P}^t\mathbf{V}^i \quad (5.13)$$

After performing the CSP, we get the projection matrix  $\mathbf{P}^t$ . Select the two most discriminative filter vectors and project them to each trial. This ensures the projected data having the property that the variance of the projected data contain the most relevant information for recognizing the two classes [10]. In fact, it makes the projected data of one class having the maximal variance while the projected data of the other class having the minimal variance.

Here we implement the CSP method and show its results comparing to our results using dataset 1-4 of subject A, both real movement and imagery movement data. The CSP method's principle is to simultaneously diagonalize the two covariance matrices associated with two classes. The two classes selected here is the ERD period and the ERS period, same as we input for the MCB spatial filter to maximize its ratio. We input 1 second ERD period data (about 0.5 to 1.5 second after the visual cue) as the first class and 1 second ERS period data (about 3 to 4 seconds after the visual cue) as the second class. The trial number used for training the Common Spatial Patterns is about 50 to 60 in one session, with the same data preprocessing procedures as we used in the MCB method. The results are as figure 5.2 shows.

### 5.1.4 Number of training trials

The last issue of the spatial filter is, does the filter performance increase as the input trial number increases? If so, what is the relationship between them and at least how many

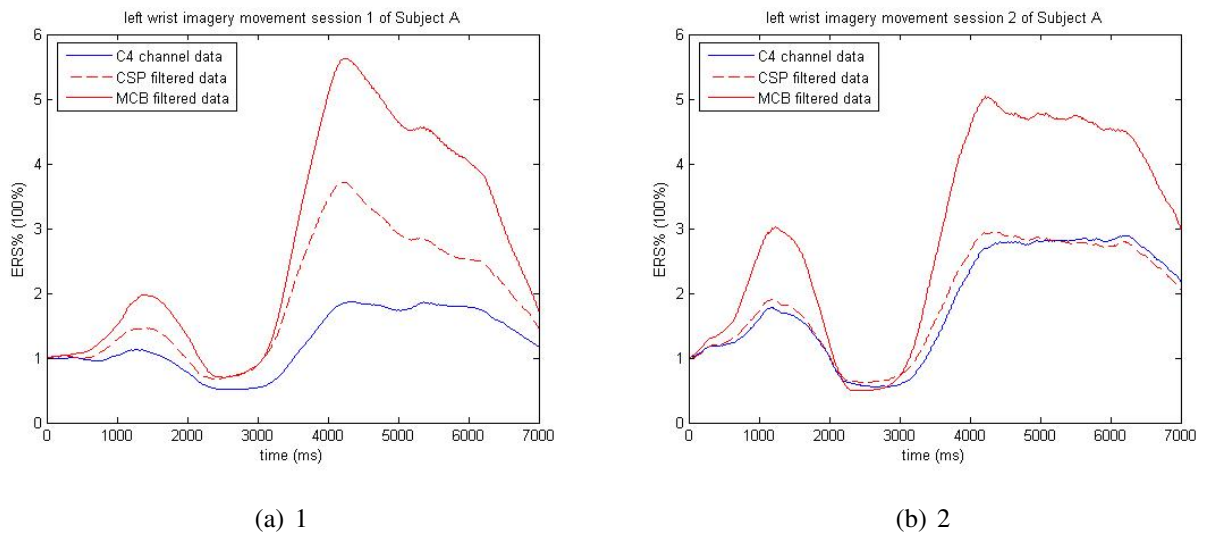


Figure 5.2: C4 channel data compared to CSP and MCB filtered data, subject A imagery session 1 and 2

trials are needed to train a spatial filter? Here we use the dataset 3 and 4 of subject A (well-trained subject) to analyze this issue. The total accepted trial number in this dataset is about 60 trials. We pick from 1 trial, 4 trials, 5 trials, 10 trials, 20 trials, 40 trials, to 60 trials and use them to train a MCB spatial filter to enhance ERD to ERS ratio. The ERS% - ERD% is used to evaluate the performance of the trained spatial filter. Table 5.1.4 and table 5.1.4 show the comparison between different trial number and the performance. Figure 5.4 uses a figure to show the same result in a better view.

The result is consistent with what we expected, that is, with the growing number of trials, the performance of the filter enhances. The ERS to ERD ratio increases. The figure also shows that when the trial number is too less, say, no more than 5 trials, the performance is unstable. And when we increase the trial number to more than 20 trials, the performance starts changing with the trial number. When the trial number is more than 40, the performance stops rising and stays good performance. According to this result, we conclude that with more trial number, we can construct a better spatial filter, and the trial number should not be less than 10 trials. Also if we want to train or retrain a spatial filter in an online feedback experiment, 40 trials should be enough to train an effective spatial filter. In the first session of our online feedback experiment, we acquire more than 40 trials. This analysis

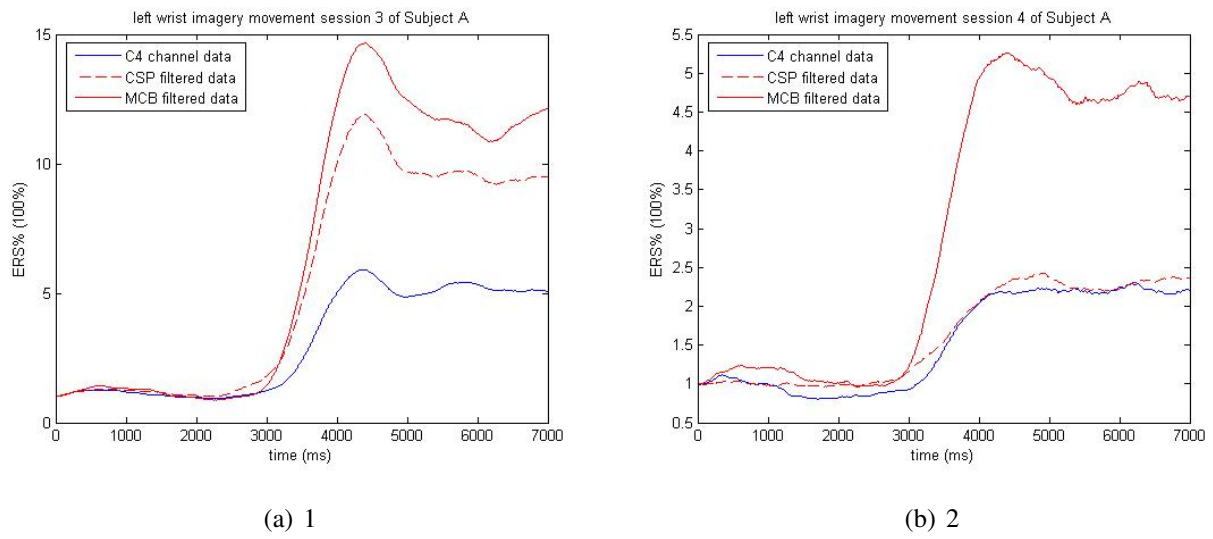


Figure 5.3: C4 channel data compared to CSP and MCB filtered data, subject A imagery session 3 and 4

supports the scheme we design.



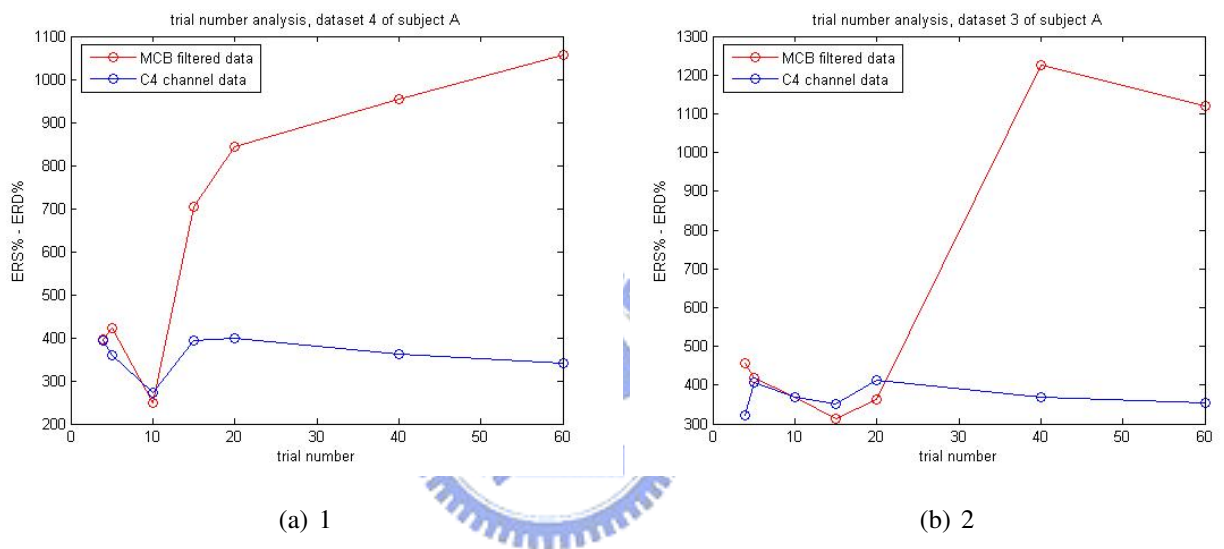


Figure 5.4: Trial number vs. filter performance. This figure uses the dataset 3 (left) and dataset 4 (right) of subject A. It shows how the filter performance changes when we use different trial number to train the filter. The X-axle is the difference between ERS% and ERD% and the Y-axle is the number of used trials. The blue line represents the C4 channel data and the red line represents the filtered data.

subject A left wrist real movement

Dataset		ERS%	ERD%	ERS%-ERD%	multiple
1	C4 channel data	296%	51%	245%	1
	ERD vs. ERS	518%	51%	467%	1.90
	resting vs. ERS	568%	57%	511%	2.08
	ERD vs. resting	230%	45%	185%	0.75
2	C4 channel data	376%	51%	325%	1
	ERD vs. ERS	671%	46%	625%	1.92
	resting vs. ERS	602%	48%	554%	1.70
	ERD vs. resting	161%	45%	116%	0.35
3	C4 channel data	439%	97%	342%	1
	ERD vs. ERS	1157%	101%	1056%	3.08
	resting vs. ERS	1102%	98%	1004%	2.93
	ERD vs. resting	979%	104%	875%	2.55
4	C4 channel data	509%	144%	365%	1
	ERD vs. ERS	1288%	102%	1186%	3.25
	resting vs. ERS	1167%	98%	1069%	2.93
	ERD vs. resting	1074%	110%	964%	2.64

Table 5.5: Results of different selection of control/active states. This table shows the results of four real movement datasets of subject A. Each dataset has four comparisons. They are unfiltered C4 channel data, ERD as control state while ERS as active state, resting as control state while ERS as active state, and ERD as control state while resting as active state MCB filtered data. The table shows the ERS and ERD enhancement as evaluation.



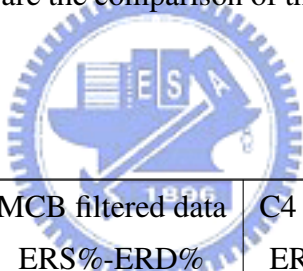
subject A left wrist imagery movement

Dataset		ERS%	ERD%	ERS%-ERD%	multiple
1	C4 channel data	181%	56%	125%	1
	ERD vs. ERS	369%	74%	295%	2.36
	resting vs. ERS	353%	73%	280%	2.24
	ERD vs. resting	122%	36%	86%	0.69
2	C4 channel data	315%	41%	274%	1
	ERD vs. ERS	398%	32%	366%	1.36
	resting vs. ERS	377%	31%	346%	1.26
	ERD vs. resting	126%	24%	102%	0.37
3	C4 channel data	447%	89%	358%	1
	ERD vs. ERS	892%	78%	814%	2.27
	resting vs. ERS	696%	75%	621%	1.73
	ERD vs. resting	967%	81%	886%	2.47
4	C4 channel data	212%	81%	131%	1
	ERD vs. ERS	408%	89%	319%	2.43
	resting vs. ERS	384%	86%	298%	2.27
	ERD vs. resting	366%	89%	277%	2.11

Table 5.6: Results of different selection of control/active states. This table shows the results of four imagery movement datasets of subject A. Each dataset has four comparisons. They are unfiltered C4 channel data, ERD as control state while ERS as active state, resting as control state while ERS as active state, and ERD as control state while resting as active state MCB filtered data. The table shows the ERS and ERD enhancement as evaluation.

trial number	MCB filtered data ERS%-ERD%	C4 channel data ERS%-ERD%
4 trials	394%	395%
5 trials	422%	360%
10 trials	249%	272%
15 trials	704%	394%
20 trials	843%	399%
40 trials	954%	361%
60 trials	1056%	342%

Table 5.7: The filter performance comparison between different number of trials. This table shows the trial number analysis using dataset 4 of subject A. The left column is the number of trials and the two right columns are the comparison of the ERS% - ERD% of the filtered data and C4 channel data.



trial number	MCB filtered data ERS%-ERD%	C4 channel data ERS%-ERD%
4 trials	456%	322%
5 trials	418%	408%
10 trials	370%	370%
15 trials	314%	352%
20 trials	462%	413%
40 trials	1226%	369%
60 trials	1120%	355%

Table 5.8: The filter performance comparison between different number of trials. This table shows the trial number analysis using dataset 3 of subject A. The left column is the number of trials and the two right columns are the comparison of the ERS% - ERD% of the filtered data and C4 channel data.

## 5.2 Adaptation

As we introduced in section 2.5, the adaptation issue can be separated into two issues. The subject adapts to the system and the system adapts to the subject. In this work we use a visual feedback to study the subject's adaptation to the system. Then we use the two session experiment, in which we train a spatial filter in the first session and online apply it in the second one, to observe the system's adaptation to the subjects.

### 5.2.1 The system to user adaptation

In the best case, the learning of the machine should be constantly proceeding. This issue is online adaptation. It is a difficult question to design a proper online adaptation scheme. According to some works studying the adaptations [16], the brief training session before the online test should be enough to obtain good performance. In our previous discussion, we show the stability of the MCB spatial filter. This supports the idea of the study.

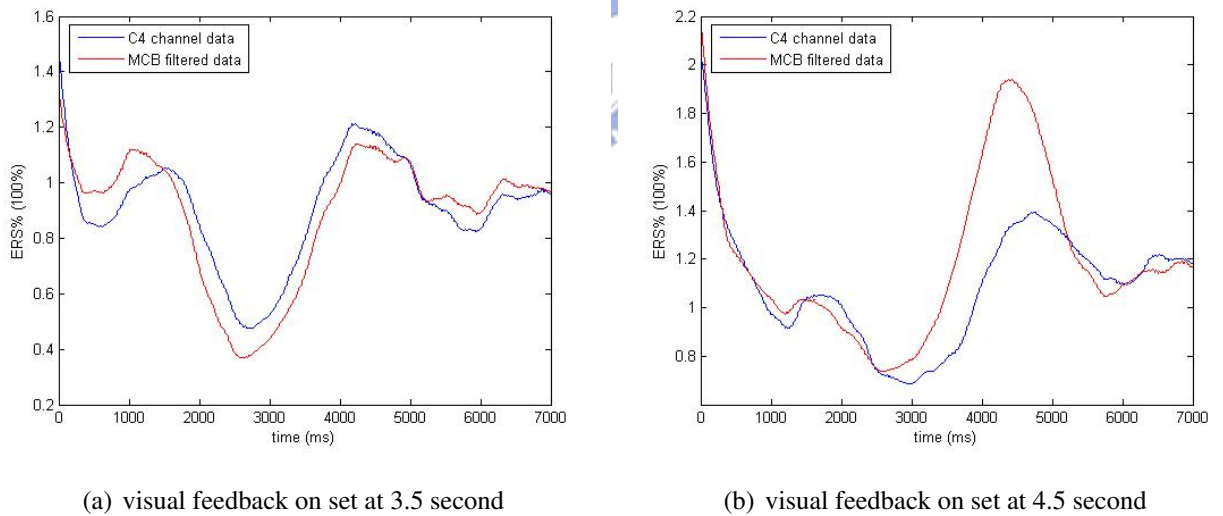


Figure 5.5: Results of different onset time of the visual feedback. The visual feedback onset time is 3.5 second in the left figure and 4.5 second in the right figure. The visual cue indicating the imagery starts at 2 second.

In the analysis of our online feedback session, we find the pre-trained spatial filter still works in the online session. The ERS% and the ERD% power changes are enhanced.

Somehow the performance is not as the offline session, but it's about the visual feedback. We discuss this next.

### 5.2.2 The user to system adaptation

We use the visual feedback to study this issue. As we introduced in chapter 2 the feedback could be both beneficial and harmful. The original thoughts to design this visual feedback is to let the user monitor the enhanced post-movement ERS. Therefore comparing to the resting period, the users may be more concentrated and train himself to obtain higher ERS.

However, according to the result, we find the visual feedback breaks the alpha band ERS. The very possible explanation is that the ERS period is seen as a recovery period after the motor imagery. When we give a visual feedback right after the recovery, our brain has a new stimulus and starts to process it. Therefore the recovery stops. We've tried few different time points of the visual feedback onset. We find it consistent that the ERS stops at the onset time of the visual feedback. As figure 5.5 shows. The left figure has the visual feedback onset at 3.5 second, and the right figure has it onset at 4.5 second. We find poor ERS in the 3.5 second case.

From this study we want to enhance the ERD and ERS power change and detect this pattern. But the visual feedback somehow breaks this scheme at the ERS stage. The previous discussion tells that we may keep moving back the onset time of visual feedback. This should works, but the meaning of the feedback should be reconsidered since the feedback is not so real-time.

## 5.3 Limitations

Here we list the limitations in this work.

### Cue-based vs. self-paced motor-imagery

The motor-imagery experiments can be categorized as cue-based and self-paced. In our design, we use cue-based experiments in the offline training session. As for the online

feedback session, there is still a cue as the offline does. However, in a real asynchronous BCI system, there could be no cue and the motor-imagery task is self-paced. There are few reasons we select cue-based experiments in both sessions.

First, although the cue-based and self-paced motor-imagery are to perform the same task, there exist slight differences. As I am one of the subjects, in a cue-based experiment I feel more concentrated than in a self-paced experiment, and in a self-paced experiment, "when to perform the task" always distracts my attention. Second, in a cue-based experiment we can always have a cue and record it with the data. After the experiment we can still analyse the data whatever we want to. But in a self-paced experiment, the timing of the imagery movement task can not be recorded. That makes it difficult to analyse the data, such as spatial filter training. Third, the design of a cue-based experiment and a self-paced experiment will be strongly different. Before we are sure about the expected result, we should not change the paradigm too much because the EEG signal is unstable.





## **Chapter 6**

### **Conclusions and Future Works**



## 6.1 Conclusions

As we describe in chapter 2. The key issues in a BCI system are noise reduction, features, classification, adaptation, and biofeedback. In this work we studied a BCI system using motor-imagery EEG. We mainly use Maximum Contrast Beamformer (MCB) technique to design a spatial filter, which has the following advantages:

1. Noise suppression

In the constraint of the MCB spatial filter, we suppress the nontarget source signal. The noise is always a big problem in a BCI system. By applying this spatial filter, we suppress the nontarget noise and focus on the cortical source activity.

2. ERD/ERS enhancement

In the constraint of the MCB spatial filter, we find the dipole orientation by maximizing the ratio between the active state and the control state. While in this work we select the during-movement ERD period as the control state and the post-movement ERS period as the active state. Therefore the ERD% and ERS% is enhanced. After the enhancement we can easily use a ROC curve analysis to evaluate the performance, which is good.

3. Stable weightings

We collect the spatial filter weightings trained in different sessions and same subject. We find them highly correlated. It means that the spatial filter is somehow stable. The same subject should be able to use the same spatial filter trained before. And a scheme like this should be workable: A subject participates an offline training session and gets his own spatial filter, then in the later online experiments we online apply this spatial filter to his data.

This spatial filter has its effectiveness because it has a hidden meaning of cortical source activity. In this work we have experiments on more than five subjects. The filtered results show good performance of this spatial filter.

In addition to the evaluation on the ERD/ERS ratio. We simply use the ROC curve to find a threshold to classify the resting state and the left wrist imagery movement state.



In this analysis we get a TPR and a FPR which shows good performance on the filtered results.

After studying the spatial filter, we implemented the online feedback system to study the online visual feedback issue. We conclude that a post-movement alpha ERS may be interrupted by a visual feedback. The further research on the online ERD/ERS detection may need to consider this visual feedback issue as a problem. In the discussion chapter we proposed some future work ideas, including the study of the visual feedback and the steady-state motor-imagery.

As for the adaptation issue, we separate this issue to two. The system's adaptation to the user and the user's adaptation to the system. We study the former issue by first evaluate the stability of the spatial filter, which has stable result. Second we design a two session experiment. In this experiment we train a spatial filter for the user in the first session. Then we apply this spatial filter online in the second session. The system should adapted to the user under this scheme. As for the latter issue, we give a visual feedback to the user in the online session. This expanding-contracting bar should be able to monitor the user's motor-imagery. The user can therefore adapt himself to the system by observing this feedback. According to our results, the visual feedback may affect the post-movement ERS. We'll have to study another way to give visual feedbacks.

## 6.2 Future works

There are many challenges in BCI systems. In the future, We should keep improving the accuracy, speed, usability and feedback methods in BCI systems. And in addition to these general challenges, here we list some future works that are related to our work.

### More than two classes

In this work we mainly analyse two classes, the resting state and the left wrist imagery movement state. In the future we may work on more than two classes. For example, left wrist movement imagery and right foot movement imagery and resting. Right now our method restricts us in only two classes, so we will have to test some more schemes if we

want to increase the classes.

### **Electrode reduction**

As we mentioned in the previous section, the electrode number we need in this work is 32, which is not a small number. One possible future work may be to analyse the relation between the filter performance and the spatial resolution. We are always happy to use less electrodes.

### **Online adaptation**

In our work we adapt the system to the user at the beginning of each online feedback session. We train a new spatial filter in the first offline session and apply it to the next. The concept is to train a new spatial filter using the data that is most similar to the online feedback session. Although in our analysis we find the spatial filter

### **Classification**

In this work we did not focus much on the classification issue in this work, in the future we can test more classification methods on the filtered data.

### **Filter templates**

Our results show that every subject has his or her own type of spatial filter weighting. In the future, if we have much more subjects participate in these experiments, and we analyse their MCB spatial filter weightings. With this large amount of data we may use some techniques like the Principle Component Analysis (PCA) to construct some filter weighting templates.

### **More applications**

In our work we did not implement the whole procedure as a communication or control system, like a typing system or a cursor control system. We mainly focus on the effectiveness analysis of the MCB spatial filter and the adaptation issue along with the online visual

feedback issue. Recall the results of our online feedback experiments, we find that the visual feedback somehow affects the post-movement power increase (ERS), and that actually restricts us. We can not just simply apply the same scheme as the online feedback session because although the spatial filter still works to enhance the ERD to ERS ratio, it's not so explicit as the offline analysis session. Due to this feedback issue suppresses the ERS, next step we will try to focus on the steady-state motor imagery.





# Bibliography

- [1] H. Cox, R. M. Zeskind, and M. M. Owen. Robust adaptive beamforming. *IEEE Trans. Acoust., Speech, Signal Processing*, ASSP-35(10):1365–1376, October 1987.
- [2] E. Donchin, K. M. Spencer, and R. Wijesinghe. The mental prosthesis: Assessing the speed of a p300-based brain-computer interface. *IEEE Transactions on Rehabilitation Engineering*, 8(2):174–179, 2000.
- [3] E. Donchin, K. M. Spencer, and R. Wijesinghe. The mental prosthesis: Assessing the speed of a p300-based brain-computer interface. *IEEE Transactions on IEEE Engineering*, 8(2):174–179, 2000.
- [4] Purves et al. *Life: The Science of Biology, 4th Edition*. Sinauer Associates & WH Freeman.
- [5] <http://faculty.washington.edu/chudler/1020.html>. 10-20 system.
- [6] <http://www.adam.com/>. Brain lobes.
- [7] H. Krim and M. Viberg. Two decades of array signal processing research. *IEEE Signal Proc. Mag.*, pages 67–94, July 1996.
- [8] A. Kubler, N. Neumann, J. Kaiser, B. Kotchoubey, T. Hinterberger, and N. P. Birbaumer. Brain-computer communication: self-regulation of slow cortical potentials for verbal communication. *Arch Phys Med Rehabil*, 82(11):1533–9, 2001. 0003-9993 (Print) Case Reports Journal Article Research Support, Non-U.S. Gov't.
- [9] E. C. Lalor, S. P. Kelly, C. Finucane, R. Burke, R. Smith, R. B. Reilly, and G. McDarby. Steady-state vep-based brain-computer interface control in an immersive 3d

- gaming environment. *Eurasip Journal on Applied Signal Processing*, 2005(19):3156–3164, 2005.
- [10] Johannes Müller-Gerking, G. Pfurtscheller, and Henrik Flyvbjerg. Designing optimal spatial filters for single-trial EEG classification in a movement task. *Clinical Neurophysiology*, 110:787–798, 1999.
- [11] J. Müller-Gerking, G. Pfurtscheller, and H. Flyvbjerg. Designing optimal spatial filters for single-trial eeg classification in a movement task. *Clinical Neurophysiology*, 110(5):787–798, 1999.
- [12] C. Neuper and G. Pfurtscheller. Evidence for distinct beta resonance frequencies in human eeg related to specific sensorimotor cortical areas. *Clin Neurophysiol*, 112(11):2084–97, 2001. 1388-2457 (Print) Comparative Study Journal Article Research Support, Non-U.S. Gov't.
- [13] G. Pfurtscheller, R. Leeb, C. Keinrath, D. Friedman, C. Neuper, C. Guger, and M. Slaterc. Walking from thought. *Brain Research*, 1071(1):145–152, 2006.
- [14] G. Pfurtscheller and F. H. Lopes da Silva. Event-related eeg/meg synchronization and desynchronization: basic principles. *Clin Neurophysiol*, 110(11):1842–57, 1999. 1388-2457 (Print) Journal Article Research Support, Non-U.S. Gov't Review.
- [15] G. Pfurtscheller, C. Neuper, C. Guger, W. Harkam, H. Ramoser, A. Schlogl, B. Obermaier, and M. Pregenzer. Current trends in graz brain-computer interface (bci) research. *IEEE Trans Rehabil Eng*, 8(2):216–9, 2000. 1063-6528 (Print) Journal Article Research Support, Non-U.S. Gov't.
- [16] P. Shenoy, M. Krauledat, B. Blankertz, R. P. Rao, and K. R. Müller. Towards adaptive classification for bci. *J Neural Eng*, 3(1):R13–23, 2006. 1741-2560 (Print) Journal Article Research Support, Non-U.S. Gov't Research Support, U.S. Gov't, Non-P.H.S.
- [17] G. Townsend, B. Graimann, and G. Pfurtscheller. Continuous eeg classification during motor imagery—simulation of an asynchronous bci. *IEEE Trans Neural Syst Rehabil Eng*, 12(2):258–65, 2004. 1534-4320 (Print) Clinical Trial Journal Article.

- [18] B. D. Van Veen, W. V. Dronghen, M. Yuchtman, and Akifumi Suzuki. Localization of brain electrical activity via linearly constrained minimum variance spatial filtering. *IEEE Transactions on Biomedical Engineering*, 44:867–880, 1997.

